An Exact Consistent Tangent Stiffness Matrix for a Second Gradient Model for Porous Plastic Solids: Derivation and Assessment.

Koffi Enakoutsa[1,2]

[1] *Department of Mathematics, California State University, Northridge, 18111 Nordhoff St, Northridge, CA 91330*

[2] *Department of Mathematics, University of California Los Angeles, 520 Portola Plaza, Los Angeles, CA 90095, email: koffi@math.ucla.edu*

Abstract

It is well known that the use of a consistent tangent stiffness matrix is critical to obtain quadratic convergence of the global Newton iterations in the finite element simulations of problems involving elasto-plastic deformation of metals, especially for large scale metallic structure problems. In this paper we derive an exact consistent stiffness matrix for a porous material model, the GLPD model developed by Gologanu, Leblond, Perrin, and Devaux for ductile fracture of porous solids based on generalized continuum mechanics assumptions. Full expressions for the derivatives of the Cauchy stress tensor and the generalized moments stress tensor the model involved are provided and implemented into a finite element code. The effectiveness and robustness of the proposed tangent stiffness moduli are assessed by applying the formulation in the finite element simulations of typical ductile fracture problems. Comparisons between the performance of our stiffness matrix and the standard ones are also provided.

Keywords: GLPD model, Numerical implementation, Tangent stiffness moduli, Ductile fracture, Micromorphic model, Plasticity of metal

1. Introduction

Constitutive models involving softening all predict unlimited localization of strain and damage. This feature generates such undesired phenomena as absence of energy dissipation during crack propagation and mesh size sensitivity in finite element computations. Gurson [11]'s famous model for porous ductile materials, which was derived from approximate limit-analysis of some elementary voided cell in a plastic solid, is no exception. In this model, unlimited localization arises from the softening because of the gradual increase of the porosity.

Several proposals have been made to solve this problem. One of these, due to Leblond *et al.* [14] but based on a previous suggestion made by Pijaudier *et al.* [20] in damage of concrete, comprises adopting a nonlocal evolution equation for the porosity involving some spatial convolution of some "local porosity rate" within an otherwise unmodified Gurson model. This simple proposal has attracted the attention of several authors (Tvergaard and Needleman [26], Tvergaard and Needleman [25], Enakoutsa *et al.* [4, 3]). It was notably checked by Tvergaard and Needleman [26] that it allows to eliminate mesh size effects. Also, Enakoutsa *et al.* [4, 3] showed that with a minor modification, it leads to an excellent numerical reproduction of the results of typical experiments of ductile rupture.

One shortcoming of Leblond *et al.* [14]'s proposal, however, is that it is purely heuristic and lacks any serious theoretical justification. This was the motivation for a later, more elaborate and physically based proposal of Gologanu *et al.* [10]. These authors derived an improved variant of Gurson's model (the *GLPD model*[1]) through some refinement of this author's original homogenization procedure based on Mandel [15]'s and Hill [13]'s classical conditions of homogeneous boundary strain rate. In the approach of Gologanu *et al.* [10], the boundary velocity is assumed to be a quadratic, rather than linear, function of the coordinates. The physical idea is to account in this way for the possibility of quick variations of the macroscopic strain rate, such as encountered during strain localization, over short distances of the order of the size of the elementary cell considered. The output of the homogenization procedure is a model of "micromorphic" nature involving the second gradient of the macroscopic velocity and generalized macroscopic stresses of "moment" type (homogeneous to the product of a stress and a distance), together with some "microstructural distance" connected to the mean spacing between neighboring voids.

The numerical implementation of the GLPD model into a finite element code is quite involved as this task required to introduce extra degrees of freedom representing strains; these extra degrees of freedom will permit the calculation of the spatial derivative of the strains, but their number will increase from 2 to 6 in 2-dimensional calculations and from 6 to 9 in the 3-dimensional calculations. This will increase the CPU time for the simulations. Another difficulty lies in the necessary operation of projection onto the sophisticated yield locus the numerical algorithm involves. An implicit algorithm similar in principle to that classically used for the von Mises criterion, although much more complex in detail, is adopted for this purpose. Convergence of the global elasto-plastic iterations was difficult. To preserve the quadractic convergence rate of the global Newton iterations stiffness tangent moduli are needed. The derivation of tangent moduli is a very difficult task, especially for constitutive models with complex forms. In this paper we derive an exact consistent stiffness matrix for the GLPD model for porous materals. The derivation is based on the small strain formulation, this choice is consistent with the one adopted in many finite element codes, including Abaqus®, Ls-dyna®, Adina®, and Systus® which have demonstrated their efficiency. In Section 2 we summarize the consitutive equations of the GLPD model. Section 3

[1] GLPD: Gologanu-Leblond-Perrin-Devaux.

presents some aspects of the numerical implementation of the GLPD model into finite element codes. In Section 4 we provide the expressions for the derivatives of the Cauchy stress tensors and the generalized moments stress tensor the GLPD model involves with respect to the main field variables. We do not compute all the terms of the tangent stiffness matrix, but only the ones that are critical for the numerical implementation. Finally, Section 5 evaluates the performance of the tangent stiffness matrix toward its capacity to reach quadratic convergence in the simulations of small scales ductile fracture problems.

2. The GLPD Model

The purpose of this section is to provide a complete description of the GLPD model developed by Gologanu, Leblond, Perrin, and Devaux. The original reference [10] for the GLPD model is not easily accessible, a summary of the equations of this model is given here. A short presentation of the derivation of these equations derived from some homogenization procedure is also provided below; strictly speaking, this presentation is not indispensable, but it is useful to fully grasp the physical foundations of the GLPD model.

2.1. Generalities

In the GLPD model, internal forces are represented through some ordinary second-rank symmetric Cauchy stress tensor $\mathbf{\Sigma}$ plus some additional third-rank "moment tensor" $\mathbf{M}$ symmetric in its first two indices only[2]. (The components of $\mathbf{\Sigma}$ and $\mathbf{M}$ are interpreted in paper [10] as the average values and "moments" of the components of the microscopic stress tensor over the elementary cell considered, but this interpretation will play no role here). The components of $\mathbf{M}$ are related through the three conditions

$$M_{ijj} = 0. \tag{1}$$

(These conditions may be compared to the condition of plane stress in the theory of thin plates or shells).

The virtual power of internal forces is given by the expression

$$\mathcal{P}^{(i)} \equiv -\int_\Omega (\mathbf{\Sigma} : \mathbf{D} + \mathbf{M} \vdots \nabla\mathbf{D})\, d\Omega \tag{2}$$

where Ω denotes the domain considered, $\mathbf{D} \equiv \frac{1}{2}\left[\nabla\mathbf{V} + (\nabla\mathbf{V})^T\right]$ ($\mathbf{V}$: material velocity) the Eulerian strain rate, $\nabla\mathbf{D}$ its gradient, $\mathbf{\Sigma} : \mathbf{D}$ the double inner product $\Sigma_{ij}D_{ij}$ and $\mathbf{M} \vdots \nabla\mathbf{D}$ the triple inner product $M_{ijk}D_{ij,k}$.

The virtual power of external forces is given by

$$\mathcal{P}^{(e)} \equiv \int_{\partial\Omega} \mathbf{T}.\mathbf{V}\, dS \tag{3}$$

where $\mathbf{T}$ represents some surface traction[3].

[2]The component M_{ijk} is noted $M_{k|ij}$ in [10]'s original paper. The present notation leads to more natural-looking expressions.

[3]The general equilibrium equations and boundary conditions corresponding to the expressions (2) and (3) of the virtual powers of internal and external forces need not be given since they are not necessary for the numerical implementation.

The corresponding equilibrium equations read, in the absence of body forces and moments:

$$\Sigma_{ij,j} - M_{ijk,jk} = 0 \quad \text{in } \Omega. \tag{4}$$

The boundary conditions are complex and will not be given here. (In fact the numerical implementation of the model will require neither the equilibrium equations nor the boundary conditions, but the sole expression of the virtual power of internal forces).

The hypothesis of additivity of elastic and plastic strain rates reads

$$\left\{ \begin{array}{lcl} \mathbf{D} & \equiv & \mathbf{D}^e + \mathbf{D}^p \\ \nabla\mathbf{D} & \equiv & (\nabla\mathbf{D})^e + (\nabla\mathbf{D})^p. \end{array} \right. \tag{5}$$

The elastic and plastic parts $(\nabla\mathbf{D})^e$, $(\nabla\mathbf{D})^p$ of the gradient of the strain rate here do *not* coincide in general with the gradients $\nabla(\mathbf{D}^e)$, $\nabla(\mathbf{D}^p)$ of the elastic and plastic parts of the strain rate.

2.2. Hypoelasticity law

The elastic parts of the strain rate and its gradient are related to the rates of the stress and moment tensors through the following hypoelasticity law:

$$\left\{ \begin{array}{lcl} \dfrac{D\Sigma_{ij}}{Dt} & = & \lambda\,\delta_{ij} D^e_{kk} + 2\mu D^e_{ij} \\ \dfrac{DM_{ijk}}{Dt} & = & \dfrac{b^2}{5}\Big[\lambda\,\delta_{ij}(\nabla D)^e_{hhk} + 2\mu(\nabla D)^e_{ijk} \\ & & -2\lambda\,\delta_{ij}U^e_k - 2\mu\left(\delta_{ik}U^e_j + \delta_{jk}U^e_i\right)\Big]. \end{array} \right. \tag{6}$$

In these expressions λ and μ denote the Lamé coefficients and b the mean half-spacing between neighboring voids. (In the homogenization procedure, b is the radius of the spherical elementary cell considered). Also, $\frac{D\Sigma_{ij}}{Dt}$ and $\frac{DM_{ijk}}{Dt}$ are the Jaumann (objective) time-derivatives of Σ_{ij} and M_{ijk}, given by

$$\left\{ \begin{array}{lcl} \dfrac{D\Sigma_{ij}}{Dt} & \equiv & \dot{\Sigma}_{ij} + \Omega_{ki}\Sigma_{kj} + \Omega_{kj}\Sigma_{ik} \\ \dfrac{DM_{ijk}}{Dt} & \equiv & \dot{M}_{ijk} + \Omega_{hi}M_{hjk} + \Omega_{hj}M_{ihk} + \Omega_{hk}M_{ijh} \end{array} \right. \tag{7}$$

where $\mathbf{\Omega} \equiv \frac{1}{2}\left[\nabla\mathbf{V} - (\nabla\mathbf{V})^T\right]$ is the antisymmetric part of the velocity gradient. Finally $\mathbf{U}^e$ is a vector the value of which is fixed by equations (1) (written in rate form, $\frac{DM_{ijj}}{Dt} = 0$):

$$U^e_i = \frac{\lambda(\nabla D)^e_{hhi} + 2\mu(\nabla D)^e_{ihh}}{2\lambda + 8\mu}. \tag{8}$$

(This vector may be compared to the through-the-thickness component of the elastic strain rate in the theory of thin plates or shells, the value of which is fixed by the condition of plane stress).

2.3. Yield criterion

The plastic behavior is governed by the following Gurson-like criterion:

$$\frac{1}{\Sigma^2}\left(\Sigma^2_{eq} + \frac{Q^2}{b^2}\right) + 2p\,\cosh\left(\frac{3}{2}\frac{\Sigma_m}{\Sigma}\right) - 1 - p^2 \leq 0. \tag{9}$$

In this expression:

- $\Sigma_{eq} \equiv \left(\frac{3}{2}\mathbf{\Sigma}' : \mathbf{\Sigma}'\right)^{1/2}$ ($\mathbf{\Sigma}'$: deviator of $\mathbf{\Sigma}$) is the von Mises equivalent stress.
- $\Sigma_m \equiv \frac{1}{3}\,\mathrm{tr}\,\mathbf{\Sigma}$ is the mean stress.
- Σ represents a kind of average value of the yield stress in the heterogeneous metallic matrix, the evolution equation of which is given below.
- p is a parameter connected to the porosity (void volume fraction) f through the relation:

$$p \equiv qf^*, f^* \equiv \left\{ \begin{array}{ll} f & \text{if } f \leq f_c \\ f_c + \delta(f - f_c) & \text{if } f > f_c \end{array} \right. \tag{10}$$

  where q is *Tvergaard's parameter*, f_c the *critical porosity at the onset of coalescence of voids*, and δ (> 1) a factor describing the accelerated degradation of the material during coalescence [23, 24],

- Q^2 is a quadratic form of the components of the moment tensor given by

$$Q^2 \equiv A_I M_I + A_{II} M_{II} \quad , \quad \left\{ \begin{array}{lcl} A_I & = & 0.194 \\ A_{II} & = & 6.108 \end{array} \right. \tag{11}$$

  where M_I and M_{II} are the quadratic invariants of $\mathbf{M}$ defined by:

$$\left\{ \begin{array}{lcl} M_I & \equiv & M_{mi} M_{mi} \\ M_{II} & \equiv & \frac{3}{2} M'_{ijk} M'_{ijk}, \end{array} \right. \tag{12}$$

  $M_{mi} \equiv \frac{1}{3} M_{hhi}$ and $\mathbf{M}'$ denoting the mean and deviatoric parts of $\mathbf{M}$, taken over its first two indices.

- Again, b is the mean half-spacing between neighboring voids.

2.4. Flow rule

The plastic parts of the strain rate and its gradient are given by the flow rule associated to the criterion (9) through normality:

$$\left\{ \begin{array}{lcl} D^p_{ij} & = & H \dfrac{\partial \Phi}{\partial \Sigma_{ij}}(\mathbf{\Sigma}, \mathbf{M}, \Sigma, f) \\ (\nabla D)^p_{ijk} & = & H \dfrac{\partial \Phi}{\partial M_{ijk}}(\mathbf{\Sigma}, \mathbf{M}, \Sigma, f) + \delta_{ik} U^p_j \\ & & \qquad + \delta_{jk} U^p_i \end{array} \right\} \tag{13}$$

were as

$$H = \left\{ \begin{array}{lll} = 0 & \text{if} & \Phi(\mathbf{\Sigma}, \mathbf{M}, \Sigma, f) < 0 \\ \geq 0 & \text{if} & \Phi(\mathbf{\Sigma}, \mathbf{M}, \Sigma, f) = 0 \end{array} \right\}$$

The term $\delta_{ik} U^p_j + \delta_{jk} U^p_i$ in equation (13) represents a rigid-body motion of the elementary cell, which is left unspecified by the flow rule but fixed in practice by conditions (1). (The vector $\mathbf{U}^p$ may be compared to the through-the-thickness component of the plastic strain rate in the theory of thin plates or shells, the value of which is fixed by the condition of plane stress).

The values of the derivatives of the yield function $\Phi(\mathbf{\Sigma}, \mathbf{M}, \Sigma, f)$ in equations (13) are readily calculated to be

$$\left\{ \begin{array}{lcl} \dfrac{\partial \Phi}{\partial \Sigma_{ij}}(\mathbf{\Sigma}, \mathbf{M}, \Sigma, f) & = & 3 \dfrac{\Sigma'_{ij}}{\Sigma^2} + \dfrac{p}{\Sigma}\, \delta_{ij} \sinh\left(\dfrac{3}{2}\dfrac{\Sigma_m}{\Sigma}\right) \\ \dfrac{\partial \Phi}{\partial M_{ijk}}(\mathbf{\Sigma}, \mathbf{M}, \Sigma, f) & = & \dfrac{1}{\Sigma^2 b^2}\left(\dfrac{2}{3} A_1 \delta_{ij} M_{mk} + 3 A_2 M'_{ijk}\right) \end{array} \right\} \tag{14}$$

2.5. Evolution of internal parameters

The evolution of the porosity is governed by the classical equation resulting from approximate incompressibility of the metallic matrix:

$$\dot{f} = (1 - f)\,\mathrm{tr}\,\mathbf{D}^p. \tag{15}$$

The parameter Σ is given by

$$\Sigma \equiv \Sigma(E) \tag{16}$$

where $\Sigma(\epsilon)$ is the function which provides the yield stress of the matrix material in terms of the local equivalent cumulated plastic strain ϵ, and E represents some average value of this equivalent strain in the heterogeneous matrix. The evolution of E is governed by the following equation:

$$(1 - f)\Sigma\dot{E} = \mathbf{\Sigma} : \mathbf{D}^p + \mathbf{M} \vdots (\nabla\mathbf{D})^p. \tag{17}$$

3. Numerical implementation

The GLPD model described in Section 2 has been incorporated into the Systus® FE code developed by ESI Group. The trickiest features of the numerical implementation, which stands as an extension of those proposed by Aravas [1] and Enakoutsa *et al.* [3] for the original Gurson model, are presented here. Emphasis is mainly placed on the complex problem of projection of the (supposedly known) elastic stress predictor onto the yield locus defined by the yield function (9). (This problem will be called the *projection problem* for shortness in the sequel).

3.0.1. The GLPD model and the class of generalized standard materials

The class of *generalized standard materials*, as defined by Halphen and Nguyen [12], consists of elastic-plastic materials for which the plastic strain *plus* the internal parameters collectively obey some "extended normality rule". This class is remarkable in that as shown by Nguyen [17], for such materials, provided that the flow rule is discretized in time with an *implicit* (backward Euler) scheme, the projection problem is equivalent to minimizing some strictly convex function, which warrants existence and uniqueness of its solution.

It so happens that the GLPD model fits into the framework of generalized standard materials *for a fixed porosity*. This property is tied to the special evolution equation (17) obeyed by the hardening parameter E. The proof is provided in Enakoutsa's [4]'s thesis and is in fact a straightforward extension of that given by Enakoutsa *et al.* [3] for the original Gurson model.

This property strongly suggests adopting an *implicit* algorithm to solve the projection problem, to take advantage of the guaranteed existence and uniqueness of the solution. However, since the porosity f must not be allowed to vary for the GLPD model to be "generalized standard", it appears necessary, to benefit from this property, to use an *explicit* scheme regarding this specific parameter. Then f will be fixed during the whole calculation of the values of field quantities at time $t + \Delta t$ from their values at time t, and updated (using a discretized version of equation (15)) only at the end upon the convergence; the projection algorithm will then be exactly the same *as if* the porosity were a constant.

We shall therefore use the explicit estimate of the porosity at time $t + \Delta t$ given by

$$f(t + \Delta t) \simeq f(t) + \dot{f}(t)\Delta t, \tag{18}$$

and the explicit estimate of the parameter $p(t+\Delta t)$ resulting from there, during the whole "transition from time t to time $t+\Delta t$", but the projection algorithm developed will otherwise be fully implicit with respect to all other parameters, that is the components of the plastic strain and the plastic strain gradient and the hardening parameter E. From now on, all quantities will conventionally be denoted with a lower index $_0$ if considered at time t, and without any special symbol if considered at time $t+\Delta t$. From now on, all quantities will implicitly be considered at time $t+\Delta t$.

3.0.2. Parametrization of the yield locus

One key point of the procedure of solution of the projection problem, aimed at reducing the number of unknowns, lies in a suitable partial parametrization of the yield locus defined by the yield function (9). This parametrization is inspired from the classical one for an ellipse and obtained by looking for the maximum possible value of the quantity $\Sigma_{eq}^2 + Q^2/b^2$, namely $(1-p)^2\Sigma^2$, and then writing this quantity in the form $(1-p)^2\,\Sigma^2\cos^2\phi$ for some angle ϕ and solving the equation $\Phi(\mathbf{\Sigma},\mathbf{M},\Sigma,f)=0$ with respect to Σ_m. One thus gets

$$\left\{\begin{array}{lcl} \Sigma_{eq}^2 + \dfrac{Q^2}{b^2} & \equiv & (1-p)^2\,\Sigma^2\cos^2\phi \\ \Sigma_m & \equiv & \dfrac{2}{3}\,\Sigma\,\mathrm{sgn}(\phi)\,\mathrm{arg\,cosh}\left[1+\dfrac{(1-p)^2\sin^2\phi}{2p}\right] \end{array}\right. \quad , \quad \phi\in\left[-\frac{\pi}{2},\frac{\pi}{2}\right]. \tag{19}$$

The sign of the parameter ϕ is introduced into equation $(19)_2$ in order to allow for negative as well as positive values of Σ_m.

3.1. Solution of the projection problem for a fixed hardening parameter

Momentarily assuming the value of the current yield stress Σ to be known, the projection problem can be solved through combination of the yield criterion and the flow rule. This problem will be reduced to a system of two coupled equations on the unknowns ϕ and Σ_{eq}, which are solved numerically to get

$$\boxed{\left[\frac{6\mu}{3\lambda+2\mu}({\Sigma_m}^*-\Sigma_m)+p\,\Sigma\,\sinh\left(\frac{3}{2}\frac{\Sigma_m}{\Sigma}\right)\right]\Sigma_{eq}=p\,\Sigma\,{\Sigma_{eq}}^*\,\sinh\left(\frac{3}{2}\frac{\Sigma_m}{\Sigma}\right).} \tag{20}$$

and

$$\boxed{\Sigma_{eq}^2\left\{1+\frac{A_1{\mathcal{M}_1}^{**}}{b^2\left[\Sigma_{eq}+\frac{3\lambda+2\mu}{45\mu}A_1\left({\Sigma_{eq}}^*-\Sigma_{eq}\right)\right]^2}+\frac{A_2{\mathcal{M}_2}^{**}}{b^2\left[\Sigma_{eq}+\frac{A_2}{5}\left({\Sigma_{eq}}^*-\Sigma_{eq}\right)\right]^2}\right\}=(1-p)^2\,\Sigma^2\cos^2\phi.} \tag{21}$$

where ${\Sigma_m}^*$, ${\Sigma_{eq}}^*$, ${\mathcal{M}_1}^{**}$, and ${\mathcal{M}_2}^{**}$ are defined as in [5] .

This is the second equation of the system looked for on the unknowns ϕ and Σ_{eq}. The left-hand side depends only on Σ_{eq} and the right-hand side only on ϕ.

The simplest way to solve the system of equations (20, 21) on ϕ and Σ_{eq} may comprise using equation (20) to express Σ_{eq} as a function of ϕ, and inserting its expression into equation (21) to get an equation on the single unknown ϕ, to be solved by Newton's method. But numerical experience reveal that the convergence of the Newton iterations is then often problematic. An alternative method comprises solving equation (20) on ϕ through Newton iterations, Σ_{eq} being calculated as a function of ϕ at each step by solving equation (21) through Newton sub-iterations.

3.1.1. Iterations on the hardening parameter

The value of the current yield stress Σ has been assumed to be known up to now. In reality, it is not and must be determined iteratively. This is done using a fixed point algorithm, starting from the value at time t, solving the projection problem with this value, updating it using a discretized form of the evolution equation (17), re-solving the projection problem with the new value, etc. up to convergence.

The discretized form of equation (17) leads to the following expression of the increment of the hardening parameter E:

$$\begin{aligned} \Delta E \quad = \quad & \frac{1}{(1-f)\Sigma}\left[\frac{\Sigma'_{ij}({\Sigma'_{ij}}^{*}-\Sigma'_{ij})}{2\mu}+\frac{3\Sigma_m({\Sigma_m}^{*}-\Sigma_m)}{3\lambda+2\mu}\right. \\ & \left.+\frac{M'_{ijk}({M'_{ijk}}^{*}-M'_{ijk})}{2\mu b^2/5}+\frac{3M_{mk}({M_{mk}}^{*}-M_{mk})}{(3\lambda+2\mu)b^2/5}\right] \end{aligned} \tag{22}$$

with, here also, ${\Sigma_m}^{*}$ and ${M'_{ijk}}^{*}$ defined as in [5] .

3.1.2. Other features of the numerical implementation

The numerical implementation of the GLPD model, just like that of all second-gradient models, raises a difficulty tied to the clear necessary use of the second derivatives of the shape functions. This seems to require elements of class $\mathcal{C}^1$ which are never available in standard finite element codes. This difficulty is circumvented through some trick suggested by Gologanu *et al.* [10] themselves and used since in several works (see, for instance, Shu *et al.* [22], Forest *et al.* [9], Matsushima *et al.* [16]) for the numerical implementation of various second-gradient models. This trick comprises introducing a new nodal variable in the form of a symmetric second-rank tensor $\mathbf{W}$, replacing the gradient of the strain rate $\mathbf{D}$ by the gradient of $\mathbf{W}$ in all equations and imposing the approximate coincidence of $\mathbf{W}$ and $\mathbf{D}$ at the Gauss points through some penalty method.

The advantage is that the components of $\nabla\mathbf{D}$ are then got from the nodal values of the new variable $\mathbf{W}$ and the sole first derivatives of the shape functions; thus, classical elements of class $\mathcal{C}^0$ are sufficient. The price to pay is an increased number of nodal degrees of freedom: six $(V_1, V_2, W_{11}, W_{22}, W_{12}, W_{33})$ instead of two (V_1, V_2) in 2D. Also, imposing the internal constraints $W_{ij} - D_{ij} = 0$ by a penalty method may give rise to locking phenomena, for which sub integration is there natural remedy. In practice, 8-node quadratic elements are used with 4-Gauss points integration. Numerical experience reveals that this suffices to prevent locking.

4. Derivation of the tangent stiffness matrix of the GLPD model

In this section we derive the equations of the tangent stiffness matrix to circumvent global Newton iterations convergence problems the numerical simulations with the GLPD model have revealed. We do not compute all the terms of this matrix but only the most important ones. Thus, we do not take into account the variations of the stresses due to the variations of the temperature; this is strictly licit because the correction of the stresses is perfomed with explicit scheme, using the stresses at time t and not at time $t + \Delta t$; and as a conseqence, the correction is independent upon the displacement increment $\Delta\mathbf{U}$ between these instants.

Also, we do not take into account the variations of the stresses due to the objective derivation in the law of hypoelasticity, which does indeed depend on $\Delta\mathbf{U}$ and therefore generates theoretically a contribution in the stiffness matrix. Similarly, the influence of geometry on the residual forces will not be taken into account. We can summarize all this by saying that the calculation of the tangent stiffness matrix will be carried out by neglecting the effects of large deformations. This choice is in conformity with the standard one used in many finite element codes for the calculation of the tangent stiffness matrix for usual elasto-plasticity models (without damage) which practical numerical simulations involing these models has demonstrated the robustness.

We assume that

$$\left\{\begin{array}{l} \tilde{\Sigma}^\star = \dfrac{\Sigma^\star}{\bar{\Sigma}} \quad ; \quad \tilde{\Sigma} = \dfrac{\mathbf{\Sigma}}{\bar{\Sigma}} \\ \\ \tilde{\mathbf{M}}^\star = \dfrac{\mathbf{M}^\star}{\bar{\Sigma}} \quad ; \quad \tilde{\mathbf{M}}^{\star\star} = \dfrac{\mathbf{M}^{\star\star}}{\bar{\Sigma}} \quad ; \quad \tilde{\mathbf{M}} \;=\; \dfrac{\mathbf{M}}{\bar{\Sigma}} \\ \\ \tilde{\mathbf{U}} = \bar{\Sigma}^2 b^2 \dfrac{\Sigma^\star_{eq} - \Sigma_{eq}}{\Sigma_{eq}} \dfrac{\mathbf{U}}{\bar{\Sigma}}. \end{array}\right. \tag{23}$$

Hence, we can rewrite the equations giving the expresions $\mathbf{U}$, Σ_{eq} and φ. With these notations, we have:

$$\left\{\begin{array}{l} \tilde{M^{\star\star}_{ijk}}' = \tilde{M^{\star}_{ijk}}' - \dfrac{1}{15}\left(\tilde{U}_j\delta_{ik} + \tilde{U}_i\delta_{jk} - \dfrac{2}{3}\tilde{U}_k\delta_{ij}\right) \\ \\ \tilde{M}^{\star\star}_{mk} = \tilde{M}^{\star}_{mk} - \dfrac{3\lambda+2\mu}{45\mu}\tilde{U}_k \end{array}\right. \tag{24}$$

and

$$\tilde{U}_i = \frac{\dfrac{\tilde{M^{\star}_{ijj}}'}{\tilde{\Sigma}_{eq} + \dfrac{A_{II}}{5}(\tilde{\Sigma}^\star_{eq} - \tilde{\Sigma}_{eq})} + \dfrac{\tilde{M}^{\star}_{mi}}{\tilde{\Sigma}_{eq} + \dfrac{3\lambda+2\mu}{45\mu}A_I(\tilde{\Sigma}^\star_{eq} - \tilde{\Sigma}_{eq})}}{\dfrac{2}{9(\tilde{\Sigma}_{eq} + \dfrac{A_{II}}{5}(\tilde{\Sigma}^\star_{eq} - \tilde{\Sigma}_{eq})} + \dfrac{\dfrac{3\lambda+2\mu}{9\mu}}{\tilde{\Sigma}_{eq} + \dfrac{3\lambda+2\mu}{9\mu}A_I(\tilde{\Sigma}^\star_{eq} - \tilde{\Sigma}_{eq})}} \equiv \tilde{U}_i(\tilde{\Sigma}_{eq}, \tilde{\Sigma}^\star, \tilde{\mathbf{M}}^\star). \tag{25}$$

The value of $\tilde{U}_i$ depends on φ through its arguments $\tilde{\Sigma}_{eq}$, $\tilde{\Sigma}^\star$, and $\tilde{\mathbf{M}}^\star$. Moreover, the equations to be solved on $\tilde{\Sigma}_{eq}$ and φ are expressed as

$$\tilde{\Sigma}_{eq}\left[1 + \frac{A_I\tilde{M}^{\star\star}_I}{b^2\left(\tilde{\Sigma}_{eq} + \dfrac{3\lambda+2\mu}{45\mu}A_I(\tilde{\Sigma}^\star_{eq} - \tilde{\Sigma}_{eq})\right)^2} + \frac{A_{II}M^{\star\star}_{II}}{b^2\left(\tilde{\Sigma}_{eq} + \dfrac{A_{II}}{5}(\tilde{\Sigma}^\star_{eq} - \tilde{\Sigma}_{eq})\right)^2}\right]^{\frac{1}{2}} - (1-p)\cos\varphi = 0$$

and

$$\frac{6\mu}{3\lambda+2\mu}(\tilde{\Sigma}^\star_m - \tilde{\Sigma}_m)\tilde{\Sigma}_{eq} - p(\tilde{\Sigma}^\star_{eq} - \tilde{\Sigma}_{eq})\sinh\left(\frac{3}{2}\tilde{\Sigma}_m\right) = 0. \tag{26}$$

In the subsequent, we introduce the following expressions:

$$\begin{cases} \mathrm{G} &= \tilde{\Sigma}_{eq}\left(1+\dfrac{A_I\tilde{M}_I^{\star\star}}{b^2\left(\tilde{\Sigma}_{eq}+\dfrac{3\lambda+2\mu}{45\mu}A_I(\tilde{\Sigma}_{eq}^{\star}-\tilde{\Sigma}_{eq})\right)^2}+\dfrac{A_{II}\tilde{M}_{II}^{\star\star}}{b^2\left(\tilde{\Sigma}_{eq}+\dfrac{A_{II}}{5}(\tilde{\Sigma}_{eq}^{\star}-\tilde{\Sigma}_{eq})\right)^2}\right)^{\frac{1}{2}} \\ &- (1-p)\cos\varphi \\ \mathrm{F} &= \dfrac{6\mu}{3\lambda+2\mu}(\tilde{\Sigma}_m^{\star}-\tilde{\Sigma}_m)\tilde{\Sigma}_{eq}-p(\tilde{\Sigma}_{eq}^{\star}-\tilde{\Sigma}_{eq})\sinh\left(\frac{3}{2}\tilde{\Sigma}_m\right) \end{cases} \tag{27}$$

where the terms G and F depend on φ, $\tilde{\Sigma}_{eq}$, $\tilde{\mathbf{\Sigma}}^{\star}$, $\tilde{\mathbf{M}}^{\star}$ and φ, $\tilde{\mathbf{\Sigma}}^{\star}$, $\tilde{\mathbf{M}}^{\star}$.

Also, let us assume that

$$\begin{cases} \mathcal{D}_1 = \tilde{\Sigma}_{eq}+\dfrac{3\lambda+2\mu}{45\mu}A_I\left(\tilde{\Sigma}_{eq}^{\star}-\tilde{\Sigma}_{eq}\right) \quad \equiv \quad \mathcal{D}_1(\tilde{\Sigma}_{eq},\tilde{\mathbf{\Sigma}}^{\star}) \\ \mathcal{D}_2 = \tilde{\Sigma}_{eq}+\dfrac{A_{II}}{45}\left(\tilde{\Sigma}_{eq}^{\star}-\tilde{\Sigma}_{eq}\right) \quad \equiv \quad \mathcal{D}_2(\tilde{\Sigma}_{eq},\tilde{\mathbf{\Sigma}}^{\star}) \\ \mathcal{D} = \dfrac{2}{9}\dfrac{1}{\mathcal{D}_2}+\dfrac{3\lambda+2\mu}{45\mu}\dfrac{1}{\mathcal{D}_1} \quad \equiv \quad \mathcal{D}(\tilde{\Sigma}_{eq},\tilde{\mathbf{\Sigma}}^{\star}). \end{cases} \tag{28}$$

Then we get

$$\tilde{U}_i = \frac{1}{\mathcal{D}}\left(\frac{\tilde{M}_{ijj}^{\star\,\prime}}{\mathcal{D}_2}+\frac{\tilde{M}_{mi}^{\star}}{\mathcal{D}_1}\right). \tag{29}$$

With Eq.(29) we write the expression for the term $\mathbf{G}$ as:

$$\mathrm{G} = \tilde{\Sigma}_{eq}\left(1+\frac{A_I\tilde{M}_I^{\star\star}}{b^2\mathcal{D}_1^2}+\frac{A_{II}\tilde{M}_{II}^{\star\star}}{b^2\mathcal{D}_2^2}\right)^{\frac{1}{2}}-(1-p)\cos\varphi. \tag{30}$$

4.1. Calculation of the derivatives

First, for practical purposes, we find the following intermediate expressions:

$$\begin{cases} \dfrac{\partial\tilde{\Sigma}_{eq}^{\star}}{\partial\tilde{\Sigma}_{ij}^{\star}} &= \dfrac{3}{2}\dfrac{\tilde{\Sigma}_{ij}^{\star\,\prime}}{\tilde{\Sigma}_{eq}^{\star}} \\ \tilde{M}_{mk}^{\star} &= \dfrac{1}{3}\tilde{M}_{hhk}^{\star} \Rightarrow \dfrac{\partial\tilde{M}_{mk}^{\star}}{\partial\tilde{M}_{pqr}} = \dfrac{1}{3}\delta_{pq}\delta_{kr} \\ \tilde{M}_{ijj}^{\star\,\prime} &= \tilde{M}_{ijj}^{\star}-\dfrac{1}{3}\delta_{ij}\tilde{M}_{hhj}^{\star} = \tilde{M}_{ijj}^{\star}-\dfrac{1}{3}\tilde{M}_{hhi}^{\star} \\ \Rightarrow \dfrac{\partial\tilde{M}_{ijj}^{\star\,\prime}}{\partial\tilde{M}_{pqr}^{\star\,\prime}} &= \dfrac{1}{2}\left(\delta_{ip}\delta_{jq}+\delta_{iq}\delta_{jp}\right)\delta_{jr}-\dfrac{1}{3}\delta_{pq}\delta_{ir} \\ &= \dfrac{1}{2}\delta_{ip}\delta_{qr}+\dfrac{1}{2}\delta_{iq}\delta_{pr}-\dfrac{1}{3}\delta_{pq}\delta_{ir}, \end{cases}$$

$$
\left\{
\begin{array}{l}
\dfrac{\partial \mathcal{D}_1}{\partial \tilde{\Sigma}_{eq}} = 1 - \dfrac{3\lambda + 2\mu}{45\mu} A_I \quad ; \quad \dfrac{\partial \mathcal{D}_2}{\partial \tilde{\Sigma}_{eq}} = 1 - \dfrac{A_{II}}{5} \\[2ex]
\dfrac{\partial \mathcal{D}_1}{\partial \tilde{\Sigma}^\star_{pq}} = \dfrac{3\lambda + 2\mu}{45\mu} A_I \dfrac{3}{2} \dfrac{\tilde{\Sigma^\star_{pq}}'}{\tilde{\Sigma}^\star_{eq}} \quad ; \quad \dfrac{\partial \mathcal{D}_2}{\partial \tilde{\Sigma}^\star_{pq}} = \dfrac{A_{II}}{5} \dfrac{3}{2} \dfrac{\tilde{\Sigma^\star_{pq}}'}{\tilde{\Sigma}^\star_{eq}} \\[2ex]
\dfrac{\partial \mathcal{D}}{\partial \tilde{\Sigma}_{eq}} = -\dfrac{3\lambda + 2\mu}{45\mu} \dfrac{1}{\mathcal{D}_1^2} \dfrac{\partial \mathcal{D}_1}{\partial \tilde{\Sigma}_{eq}} - \dfrac{2}{9} \dfrac{1}{\mathcal{D}_2^2} \dfrac{\partial \mathcal{D}_2}{\partial \tilde{\Sigma}_{eq}} \\[2ex]
\dfrac{\partial \mathcal{D}}{\partial \tilde{\Sigma}^\star_{pq}} = -\dfrac{3\lambda + 2\mu}{45\mu} \dfrac{1}{\mathcal{D}_1^2} \dfrac{\partial \mathcal{D}_1}{\partial \tilde{\Sigma}_{pq}} - \dfrac{2}{9} \dfrac{1}{\mathcal{D}_2^2} \dfrac{\partial \mathcal{D}_2}{\partial \tilde{\Sigma}_{pq}}.
\end{array}
\right. \tag{31}
$$

4.1.1. Derivatives of the $\tilde{U}_i$

The terms $\tilde{U}_i$ depends on $\tilde{\Sigma}_{eq}$, $\tilde{\mathbf{\Sigma}}^\star$ et $\tilde{\mathbf{M}}^\star$; as a consequence, we have

$$
\begin{array}{rcl}
\dfrac{\partial \tilde{U}_i}{\partial \tilde{\Sigma}_{eq}} &=& -\dfrac{1}{\mathcal{D}^2} \dfrac{\partial \mathcal{D}}{\partial \tilde{\Sigma}_{eq}} \left(\dfrac{\tilde{M^\star_{ijj}}'}{\mathcal{D}_2} + \dfrac{\tilde{M}^\star_{mi}}{\mathcal{D}_1} \right) - \dfrac{1}{\mathcal{D}} \left(\dfrac{\tilde{M^\star_{ijj}}'}{\mathcal{D}_2^2} \dfrac{\partial \mathcal{D}_2}{\partial \tilde{\Sigma}_{eq}} + \dfrac{\tilde{M}^\star_{mi}}{\mathcal{D}_1^2} \dfrac{\partial \mathcal{D}_1}{\partial \tilde{\Sigma}_{eq}} \right) \\[2ex]
&=& -\left(\dfrac{1}{\mathcal{D}^2 \mathcal{D}_2} \dfrac{\partial \mathcal{D}}{\partial \tilde{\Sigma}_{eq}} + \dfrac{1}{\mathcal{D} \mathcal{D}_2^2} \dfrac{\partial \mathcal{D}_2}{\partial \tilde{\Sigma}_{eq}} \right) \tilde{M^\star_{ijj}}' - \left(\dfrac{1}{\mathcal{D}^2 \mathcal{D}_1} \dfrac{\partial \mathcal{D}}{\partial \tilde{\Sigma}_{eq}} + \dfrac{1}{\mathcal{D} \mathcal{D}_1^2} \dfrac{\partial \mathcal{D}_1}{\partial \tilde{\Sigma}_{eq}} \right) \tilde{M}^\star_{mi} \quad ; \\[2ex]
\dfrac{\partial \tilde{U}_i}{\partial \tilde{\Sigma}^\star_{pq}} &=& -\left(\dfrac{1}{\mathcal{D}^2 \mathcal{D}_2} \dfrac{\partial \mathcal{D}}{\partial \tilde{\Sigma}^\star_{pq}} + \dfrac{1}{\mathcal{D} \mathcal{D}_2^2} \dfrac{\partial \mathcal{D}_2}{\partial \tilde{\Sigma}^\star_{pq}} \right) \tilde{M^\star_{ijj}}' - \left(\dfrac{1}{\mathcal{D}^2 \mathcal{D}_1} \dfrac{\partial \mathcal{D}}{\Sigma_{pq}} + \dfrac{1}{\mathcal{D} \mathcal{D}_1^2} \dfrac{\partial \mathcal{D}_1}{\partial \tilde{\Sigma}^\star_{pq}} \right) \tilde{M}^\star_{mi} \quad \text{and} \\[2ex]
\dfrac{\partial \tilde{U}_i}{\partial \tilde{M}^\star_{pqr}} &=& \dfrac{1}{\mathcal{D}} \left(\dfrac{1}{\mathcal{D}_1} \dfrac{\partial \tilde{M}^\star_{mi}}{\partial \tilde{M}^\star_{pqr}} + \dfrac{1}{\mathcal{D}_2} \dfrac{\partial \tilde{M}^\star_{ijj}}{\partial \tilde{M}^\star_{pqr}} \right) \\[2ex]
&=& \dfrac{1}{\mathcal{D}} \left[\dfrac{1}{\mathcal{D}_1} \dfrac{1}{3} \delta_{pq} \delta_{ir} + \dfrac{1}{\mathcal{D}_2} \left(\dfrac{1}{2} \delta_{ip} \delta_{qr} + \dfrac{1}{2} \delta_{iq} \delta_{pr} - \dfrac{1}{3} \delta_{pq} \delta_{ir} \right) \right].
\end{array}
$$

4.1.2. The derivatives of the terms $\tilde{M^{\star\star}_{ijk}}'$ and $\tilde{M}^{\star\star}_{mk}$

The terms $\tilde{M^{\star\star}_{ijk}}'$ and $\tilde{M}^{\star\star}_{mk}$ also depend on $(\tilde{\Sigma}_{eq}, \tilde{\mathbf{\Sigma}}^\star, \tilde{\mathbf{M}}^\star)$; thus we get

$$
\left\{
\begin{array}{rcl}
\dfrac{\partial \tilde{M^{\star\star}_{ijk}}'}{\partial \tilde{\Sigma}_{eq}} &=& -\dfrac{1}{15} \left(\dfrac{\partial \tilde{U}_j}{\partial \tilde{\Sigma}_{eq}} \delta_{ik} + \dfrac{\partial \tilde{U}_i}{\partial \tilde{\Sigma}_{eq}} \delta_{jk} - \dfrac{2}{3} \dfrac{\partial \tilde{U}_k}{\partial \tilde{\Sigma}_{eq}} \delta_{ij} \right) \\[2ex]
\dfrac{\partial \tilde{M}^{\star\star}_{mk}}{\partial \tilde{\Sigma}_{eq}} &=& -\dfrac{3\lambda + 2\mu}{45\mu} \dfrac{\partial \tilde{U}_k}{\partial \tilde{\Sigma}_{eq}},
\end{array}
\right. \tag{32}
$$

$$\left\{\begin{array}{lcl} \dfrac{\partial \tilde{M}^{\star\star}_{ijk}{}'}{\partial \tilde{\Sigma}^{\star}_{pq}} & = & -\dfrac{1}{15}\left(\dfrac{\partial \tilde{U}_j}{\partial \tilde{\Sigma}^{\star}_{pq}}\delta_{ik}+\dfrac{\partial \tilde{U}_i}{\partial \tilde{\Sigma}^{\star}_{pq}}\delta_{jk}-\dfrac{2}{3}\dfrac{\partial \tilde{U}_k}{\partial \tilde{\Sigma}^{\star}_{pq}}\delta_{ij}\right) \\ \dfrac{\partial \tilde{M}^{\star\star}_{mk}}{\partial \tilde{\Sigma}^{\star}_{pq}} & = & -\dfrac{3\lambda+2\mu}{45\mu}\dfrac{\partial \tilde{U}_k}{\partial \tilde{\Sigma}^{\star}_{pq}} \end{array}\right. \tag{33}$$

and

$$\left\{\begin{array}{lcl} \dfrac{\partial \tilde{M}^{\star\star}_{ijk}{}'}{\partial \tilde{M}^{\star}_{pqr}} & = & \dfrac{1}{2}(\delta_{ip}\delta_{jq}+\delta_{iq}\delta_{jp})\delta_{kr}-\dfrac{1}{3}\delta_{ij}\delta_{pq}\delta_{kr} \\ & - & \dfrac{1}{15}\left(\dfrac{\partial \tilde{U}_j}{\partial \tilde{M}^{\star}_{pqr}}\delta_{ik}+\dfrac{\partial \tilde{U}_i}{\partial \tilde{M}^{\star}_{pqr}}\delta_{jk}-\dfrac{2}{3}\dfrac{\partial \tilde{U}_k}{\partial \tilde{M}^{\star}_{pqr}}\delta_{ij}\right) \\ \dfrac{\partial \tilde{M}^{\star\star}_{mk}}{\partial \tilde{M}^{\star}_{pqr}} & = & \dfrac{1}{3}\delta_{pq}\delta_{kr}-\dfrac{3\lambda+2\mu}{45\mu}\dfrac{\partial \tilde{U}_k}{\partial \tilde{M}^{\star}_{pqr}}. \end{array}\right. \tag{34}$$

4.1.3. The derivatives of $\tilde{M}^{\star\star}_{I}$ and $\tilde{M}^{\star\star}_{II}$

The terms $\tilde{M}^{\star\star}_{I}$ and $\tilde{M}^{\star\star}_{II}$ depend on the variables $(\tilde{\Sigma}_{eq}, \tilde{\mathbf{\Sigma}}^{\star}, \tilde{\mathbf{M}}^{\star})$. Taking the derivatives we get

$$\left\{\begin{array}{l} \tilde{M}^{\star\star}_{I}=\dfrac{1}{9}\tilde{M}^{\star\star}_{hhi}\tilde{M}^{\star\star}_{kki} \quad \Rightarrow \quad \dfrac{\partial \tilde{M}^{\star\star}_{I}}{\partial \tilde{\Sigma}_{eq}}=\dfrac{2}{9}\tilde{M}^{\star\star}_{kki}\dfrac{\partial \tilde{M}^{\star\star}_{hhi}}{\partial \tilde{\Sigma}_{eq}}=2\tilde{M}^{\star\star}_{mk}\dfrac{\partial \tilde{M}^{\star\star}_{mk}}{\partial \tilde{\Sigma}_{eq}} \\ \tilde{M}^{\star\star}_{II}=\dfrac{3}{2}\tilde{M}^{\star\star}_{ijk}{}'\tilde{M}^{\star\star}_{ijk}{}' \quad \Rightarrow \quad \dfrac{\partial \tilde{M}^{\star\star}_{II}}{\partial \tilde{\Sigma}_{eq}}=3\tilde{M}^{\star\star}_{ijk}{}'\dfrac{\partial \tilde{M}^{\star\star}_{ijk}{}'}{\partial \tilde{\Sigma}_{eq}}=-\dfrac{2}{5}\tilde{M}^{\star\star}_{ijj}{}'\dfrac{\partial \tilde{U}_i}{\partial \tilde{\Sigma}_{eq}}, \end{array}\right. \tag{35}$$

$$\left\{\begin{array}{l} \dfrac{\partial \tilde{M}^{\star\star}_{I}}{\partial \tilde{\Sigma}^{\star}_{pq}}=\dfrac{2}{9}\tilde{M}^{\star\star}_{hhi}\dfrac{\partial \tilde{M}^{\star\star}_{kki}}{\partial \tilde{\Sigma}^{\star}_{pq}}=2\tilde{M}^{\star\star}_{mk}\dfrac{\partial \tilde{M}^{\star\star}_{mk}}{\partial \tilde{\Sigma}^{\star}_{pq}} \\ \dfrac{\partial \tilde{M}^{\star\star}_{II}}{\partial \tilde{\Sigma}^{\star}_{pq}}=3\tilde{M^{\star\star}_{ijk}}{}'\dfrac{\partial \tilde{M}^{\star\star}_{ijk}{}'}{\partial \tilde{\Sigma}^{\star}_{pq}}=-\dfrac{2}{5}\tilde{M}^{\star\star}_{ijj}{}'\dfrac{\partial \tilde{U}_i}{\partial \tilde{\Sigma}^{\star}_{pq}}, \end{array}\right. \tag{36}$$

and

$$\left\{\begin{array}{l} \dfrac{\partial \tilde{M}^{\star\star}_{I}}{\partial \tilde{M}^{\star}_{pqr}}=\dfrac{2}{9}\tilde{M}^{\star\star}_{hhi}\dfrac{\partial \tilde{M}^{\star\star}_{kki}}{\partial \tilde{M}^{\star}_{pqr}}=2\tilde{M}^{\star\star}_{mk}\dfrac{\partial \tilde{M}^{\star\star}_{mk}}{\partial \tilde{M}^{\star}_{pqr}} \\ \dfrac{\partial \tilde{M}^{\star\star}_{II}}{\partial \tilde{M}^{\star}_{pqr}}=3\tilde{M}^{\star\star}_{ijk}{}'\dfrac{\partial \tilde{M}^{\star\star}_{ijk}{}'}{\partial \tilde{M}^{\star}_{pqr}}=3\tilde{M}^{\star\star}_{pqr}{}'-\dfrac{2}{5}\tilde{M}^{\star\star}_{ijj}{}'\dfrac{\partial \tilde{U}_i}{\partial \tilde{M}^{\star}_{pqr}}. \end{array}\right. \tag{37}$$

4.1.4. The derivatives of G

We know that $\mathrm{G} \equiv \mathbf{G}(\varphi, \tilde{\Sigma}_{eq}, \tilde{\mathbf{\Sigma}}^{\star}, \tilde{\mathbf{M}}^{\star})$. By posing that

$$\mathcal{S}=\left(1+\frac{A_I\tilde{M}^{\star\star}_{I}}{b^2\mathcal{D}_1^2}+\frac{A_{II}\tilde{M}^{\star\star}_{II}}{b^2\mathcal{D}_2^2}\right)^{\frac{1}{2}} \equiv \mathcal{S}(\tilde{\Sigma}_{eq}, \tilde{\mathbf{\Sigma}}^{\star}, \tilde{\mathbf{M}}^{\star}), \tag{38}$$

we get

$$\mathrm{G} = \tilde{\Sigma}_{eq}\mathcal{S} - (1-p)\cos\varphi. \tag{39}$$

Therafter, we obtain

$$\begin{cases} \dfrac{\partial \mathrm{G}}{\partial \tilde{\Sigma}_{eq}} &= \mathcal{S} + \tilde{\Sigma}_{eq}\dfrac{\partial \mathcal{S}}{\partial \tilde{\Sigma}_{eq}} \\ &= \mathcal{S} + \dfrac{\tilde{\Sigma}_{eq}}{2\mathcal{S}}\left(\dfrac{A_I}{b^2\mathcal{D}_1^2}\dfrac{\partial \tilde{M}_I^{\star\star}}{\partial \tilde{\Sigma}_{eq}} + \dfrac{A_{II}}{b^2\mathcal{D}_2^2}\dfrac{\partial \tilde{M}_{II}^{\star\star}}{\partial \tilde{\Sigma}_{eq}} - \dfrac{2A_{II}}{b^2\mathcal{D}_1^3}\tilde{M}_{II}^{\star\star}\dfrac{\partial \mathcal{D}_1}{\partial \tilde{\Sigma}_{eq}} - \dfrac{2A_{II}}{b^2\mathcal{D}_2^3}\tilde{M}_{II}^{\star\star}\dfrac{\partial \mathcal{D}_2}{\partial \tilde{\Sigma}_{eq}}\right) \\ \dfrac{\partial \mathrm{G}}{\partial \tilde{\Sigma}_{pq}^{\star}} &= \tilde{\Sigma}_{eq}\dfrac{\partial \mathcal{S}}{\partial \tilde{\Sigma}_{pq}^{\star}} \\ &= \dfrac{\tilde{\Sigma}_{eq}}{2\mathcal{S}}\left(\dfrac{A_I}{b^2\mathcal{D}_1^2}\dfrac{\partial \tilde{M}_I^{\star\star}}{\partial \tilde{\Sigma}_{pq}^{\star}} + \dfrac{A_{II}}{b^2\mathcal{D}_2^2}\dfrac{\partial \tilde{M}_{II}^{\star\star}}{\partial \tilde{\Sigma}_{pq}^{\star}} - \dfrac{2A_I}{b^2\mathcal{D}_1^3}\tilde{M}_I^{\star\star}\dfrac{\partial \mathcal{D}_1}{\partial \tilde{\Sigma}_{pq}^{\star}} - \dfrac{2A_{II}}{b^2\mathcal{D}_2^3}\tilde{M}_{II}^{\star\star}\dfrac{\partial \mathcal{D}_2}{\partial \tilde{\Sigma}_{pq}^{\star}}\right) \\ \dfrac{\partial \mathrm{G}}{\partial \tilde{M}_{pqr}^{\star}} &= \tilde{\Sigma}_{eq}\dfrac{\partial \mathcal{S}}{\partial \tilde{M}_{pqr}^{\star}} = \dfrac{\tilde{\Sigma}_{eq}}{2\mathcal{S}}\left(\dfrac{A_I}{b^2\mathcal{D}_2^2}\dfrac{\partial \tilde{M}_I^{\star\star}}{\partial \tilde{M}_{pqr}^{\star}} + \dfrac{A_{II}}{b^2\mathcal{D}_2^2}\dfrac{\partial \tilde{M}_{II}^{\star\star}}{\partial \tilde{M}_{pqr}^{\star}}\right) \\ \dfrac{\partial \mathrm{G}}{\partial \varphi} &= (1-p)\sin\varphi. \end{cases} \tag{40}$$

With the derivatives of G we can find the derivatives of $\tilde{\Sigma}_{eq}$ with respect to φ, $\tilde{\Sigma}^{\star}$, $\tilde{\mathbf{M}}^{\star}$.

4.1.5. The derivatives of the term $\tilde{\Sigma}_{eq}$ with respect to φ, $\tilde{\Sigma}^{\star}$, $\tilde{\mathbf{M}}^{\star}$

The following implications hold:

$$\begin{aligned} \mathrm{G} \equiv \mathrm{G}(\varphi, \tilde{\Sigma}_{eq}, \tilde{\mathbf{\Sigma}}^{\star}, \tilde{\mathbf{M}}^{\star}) = 0 \quad &\Rightarrow \quad \frac{\partial \mathrm{G}}{\partial \tilde{\Sigma}_{eq}} D\tilde{\Sigma}_{eq} + \frac{\partial \mathrm{G}}{\partial \varphi} D\varphi + \frac{\partial \mathbf{G}}{\partial \tilde{\Sigma}_{pq}^{\star}} D\tilde{\Sigma}_{pq}^{\star} + \frac{\partial \mathrm{G}}{\partial \tilde{M}_{pqr}^{\star}} D\tilde{M}_{pqr}^{\star} = 0 \\ &\Rightarrow \quad \frac{\partial \tilde{\Sigma}_{eq}}{\partial \varphi} = -\frac{\partial \mathrm{G}/\partial \varphi}{\partial \mathrm{G}/\partial \tilde{\Sigma}_{eq}} \quad ; \quad \frac{\partial \tilde{\Sigma}_{eq}}{\partial \tilde{\Sigma}_{pq}^{\star}} = -\frac{\partial \mathrm{G}/\partial \tilde{\Sigma}_{pq}^{\star}}{\partial \mathrm{G}/\partial \tilde{\Sigma}_{eq}}; \\ &\qquad \frac{\partial \tilde{\Sigma}_{eq}}{\partial \tilde{M}_{pqr}^{\star}} = -\frac{\partial \mathrm{G}/\partial \tilde{M}_{pqr}^{\star}}{\partial \mathrm{G}/\partial \tilde{\Sigma}_{eq}}. \end{aligned}$$

4.1.6. The derivative of $F(\varphi, \tilde{\Sigma}^\star, \tilde{\mathbf{M}}^\star)$

From the formula defining F, we immediately obtain the derivatives

$$\left\{\begin{array}{rcl} \dfrac{\partial \mathrm{F}}{\partial \varphi} & = & \left[-\dfrac{6\mu}{3\lambda+2\mu}\tilde{\Sigma}_{eq} - \dfrac{3}{2}p(\tilde{\Sigma}^\star_{eq} - \tilde{\Sigma}_{eq})\cosh(\dfrac{3}{2}\tilde{\Sigma}_m)\right]\dfrac{D\tilde{\Sigma}_m}{D\varphi} \\ & + & \left[\dfrac{6\mu}{3\lambda+2\mu}(\tilde{\Sigma}^\star_m - \tilde{\Sigma}_m) + p\sinh(\dfrac{3}{2}\tilde{\Sigma}_m)\right]\dfrac{\partial \tilde{\Sigma}_{eq}}{\partial \varphi} \\ \dfrac{\partial \mathrm{F}}{\partial \tilde{\Sigma}^\star_{pq}} & = & \dfrac{2\mu}{3\lambda+2\mu}\delta_{pq}\tilde{\Sigma}_{eq} - \dfrac{3p}{2}\sinh(\dfrac{3}{2}\tilde{\Sigma}_m)\dfrac{\tilde{\Sigma^\star_{pq}}'}{\tilde{\Sigma}^\star_{eq}} \\ & + & \left[\dfrac{6\mu}{3\lambda+2\mu}(\tilde{\Sigma}^\star_m - \tilde{\Sigma}_m) + p\sinh(\dfrac{3}{2}\tilde{\Sigma}_m)\right]\dfrac{\partial \tilde{\Sigma}_{eq}}{\partial \tilde{\Sigma}^\star_{pq}} \\ \dfrac{\partial \mathrm{F}}{\partial \tilde{M}^\star_{pqr}} & = & \left[\dfrac{6\mu}{3\lambda+2\mu}(\tilde{\Sigma}^\star_m - \tilde{\Sigma}_m) + p\sinh(\dfrac{3}{2}\tilde{\Sigma}_m)\right]\dfrac{\partial \tilde{\Sigma}_{eq}}{\partial \tilde{M}^\star_{pqr}} \end{array}\right. \tag{41}$$

which enable the calculation of the derivatives of the term φ with respect to $\tilde{\Sigma}^\star$ and $\tilde{\mathbf{M}}^\star$.

4.1.7. The derivatives of the terms $\varphi(\tilde{\Sigma}^\star, \tilde{\mathbf{M}}^\star)$

Following the results obtained in Section (4.1.6), we have

$$\begin{array}{rcl} \mathrm{F} \equiv \mathrm{F}(\varphi, \tilde{\mathbf{\Sigma}}^\star, \tilde{\mathbf{M}}^\star) = 0 & \Rightarrow & \dfrac{\partial \mathrm{F}}{\partial \varphi} D\varphi + \dfrac{\partial \mathrm{F}}{\partial \tilde{\Sigma}^\star_{pq}} D\tilde{\Sigma}^\star_{pq} + \dfrac{\partial \mathrm{F}}{\partial \tilde{M}^\star_{pqr}} D\tilde{M}^\star_{pqr} = 0 \\ & \Rightarrow & \dfrac{\partial \varphi}{\partial \tilde{\Sigma}^\star_{pq}} = -\dfrac{\partial \mathrm{F}/\partial \tilde{\Sigma}^\star_{pq}}{\partial \mathrm{F}/\partial \varphi} \quad ; \quad \dfrac{\partial \varphi}{\partial \tilde{M}^\star_{pqr}} = -\dfrac{\partial \mathrm{F}/\partial \tilde{M}^\star_{pqr}}{\partial \mathrm{F}/\partial \varphi}. \end{array}$$

4.1.8. The derivatives of $\tilde{\Sigma}_{eq}(\tilde{\Sigma}^\star, \tilde{\mathbf{M}}^\star)$

We denote the derivatives in this section by $\dfrac{D\tilde{\Sigma}_{eq}}{D\tilde{\Sigma}^\star_{pq}}$ and $\dfrac{\mathrm{D}\tilde{\Sigma}_{eq}}{D\tilde{M}^\star_{pqr}}$. We obtain

$$\left\{\begin{array}{l} \dfrac{D\tilde{\Sigma}_{eq}}{D\tilde{\Sigma}^\star_{pq}} = \dfrac{\partial \tilde{\Sigma}_{eq}}{\partial \tilde{\Sigma}^\star_{pq}} + \dfrac{\partial \tilde{\Sigma}_{eq}}{\partial \varphi}\dfrac{\partial \varphi}{\partial \tilde{\Sigma}^\star_{pq}} \\ \dfrac{D\tilde{\Sigma}_{eq}}{D\tilde{M}^\star_{pqr}} = \dfrac{\partial \tilde{\Sigma}_{eq}}{\partial \tilde{M}^\star_{pqr}} + \dfrac{\partial \tilde{\Sigma}_{eq}}{\partial \varphi}\dfrac{\partial \varphi}{\partial \tilde{M}^\star_{pqr}}. \end{array}\right. \tag{42}$$

4.1.9. The derivatives of $\tilde{\Sigma}_m(\tilde{\Sigma}^\star, \tilde{\mathbf{M}}^\star)$

We get

$$\frac{\partial \tilde{\Sigma}_m}{\partial \tilde{\Sigma}^\star_{pq}} = \frac{D\tilde{\Sigma}_m}{D\varphi}\frac{\partial \varphi}{\partial \Sigma^\star_{pq}} \quad ; \quad \frac{\partial \tilde{\Sigma}_m}{\partial \tilde{M}^\star_{pqr}} = \frac{D\tilde{\Sigma}_m}{D\varphi}\frac{\partial \varphi}{\partial M^\star_{pqr}}.$$

4.1.10. The derivatives of $\tilde{\mathbf{\Sigma}}'(\tilde{\Sigma}^\star;\tilde{\mathbf{M}}^\star)$

We find

$$\Sigma'_{ij} = \frac{\tilde{\Sigma}_{eq}}{\tilde{\Sigma}^\star_{eq}}\Sigma^{\star\,\prime}_{ij} \quad \Rightarrow \quad \frac{\partial\tilde{\Sigma}'_{ij}}{\partial\tilde{\Sigma}^\star_{pq}} = \frac{1}{\tilde{\Sigma}^\star_{eq}}\frac{D\tilde{\Sigma}_{eq}}{D\tilde{\Sigma}^\star_{pq}}\tilde{\Sigma^\star_{ij}}' - \frac{\tilde{\Sigma}_{eq}}{(\tilde{\Sigma}^\star_{eq})^2}\frac{\partial\tilde{\Sigma}^\star_{eq}}{\partial\tilde{\Sigma}^\star_{pq}}\tilde{\Sigma^\star_{ij}}' + \frac{\tilde{\Sigma}_{eq}}{\tilde{\Sigma}^\star_{eq}}\frac{\partial\tilde{\Sigma^\star_{ij}}'}{\partial\tilde{\Sigma}^\star_{pq}}$$

where

$$\begin{aligned}
\frac{\partial\tilde{\Sigma}^\star_{eq}}{\partial\tilde{\Sigma}^\star_{pq}} &= \frac{3}{2}\frac{\tilde{\Sigma^\star_{pq}}'}{\tilde{\Sigma}^\star_{eq}} \quad \text{et} \quad \frac{\partial\tilde{\Sigma^\star_{ij}}'}{\partial\tilde{\Sigma}^\star_{pq}} = \frac{1}{2}(\delta_{ip}\delta_{jq}+\delta_{iq}\delta_{jp}) - \frac{1}{3}\delta_{ij}\delta_{pq} \\
\frac{\partial\tilde{\Sigma}'_{ij}}{\partial\tilde{M}^\star_{pqr}} &= \frac{1}{\tilde{\Sigma}^\star_{eq}}\frac{D\tilde{\Sigma}_{eq}}{D\tilde{M}^\star_{pqr}}\tilde{\Sigma^\star_{ij}}'.
\end{aligned}$$

It becomes possible, from these last equations, to easily compute $\dfrac{\partial\tilde{\Sigma}_{ij}}{\partial\tilde{\Sigma}^\star_{pq}}$ and $\dfrac{\partial\tilde{\Sigma}_{ij}}{\partial\tilde{M}^\star_{pqr}}$.

4.1.11. The derivatives of the terms $\tilde{M}^{\star\star}_{mk}(\tilde{\Sigma}^\star;\tilde{\mathbf{M}}^\star)$ *and* $\tilde{M}'^{\star\star}_{ijk}(\tilde{\Sigma}^\star;\tilde{\mathbf{M}}^\star)$

The derivatives of $\tilde{M}^{\star\star}_{mk}$ are given by

$$\left\{\begin{array}{l}
\dfrac{D\tilde{M}^{\star\star}_{mk}}{D\tilde{\Sigma}^\star_{pq}} = \dfrac{\partial\tilde{M}^{\star\star}_{mk}}{\partial\tilde{\Sigma}^\star_{pq}} + \dfrac{\partial\tilde{M}^{\star\star}_{mk}}{\partial\tilde{\Sigma}_{eq}}\dfrac{D\tilde{\Sigma}_{eq}}{D\tilde{\Sigma}^\star_{pq}} \quad ; \quad \dfrac{D\tilde{M}^{\star\star}_{mk}}{D\tilde{M}^\star_{pqr}} = \dfrac{\partial\tilde{M}^{\star\star}_{mk}}{\partial\tilde{M}^\star_{pqr}} + \dfrac{\partial\tilde{M}^{\star\star}_{mk}}{\partial\tilde{\Sigma}_{eq}}\dfrac{D\tilde{\Sigma}_{eq}}{D\tilde{M}^\star_{pqr}} \\
\dfrac{D\tilde{M}^{\star\star\,\prime}_{ijk}}{D\tilde{\Sigma}^\star_{pq}} = \dfrac{\partial\tilde{M}^{\star\star\,\prime}_{ijk}}{\partial\tilde{\Sigma}^\star_{pq}} + \dfrac{\partial\tilde{M}^{\star\star\,\prime}_{ijk}}{\partial\tilde{\Sigma}_{eq}}\dfrac{D\tilde{\Sigma}_{eq}}{D\tilde{\Sigma}^\star_{pq}} \quad ; \quad \dfrac{D\tilde{M}^{\star\star\,\prime}_{ijk}}{D\tilde{M}^\star_{pqr}} = \dfrac{\partial\tilde{M}^{\star\star\,\prime}_{ijk}}{\partial\tilde{M}^\star_{pqr}} + \dfrac{\partial\tilde{M}^{\star\star\,\prime}_{ijk}}{\partial\tilde{\Sigma}_{eq}}\dfrac{D\tilde{\Sigma}_{eq}}{D\tilde{M}^\star_{pqr}}.
\end{array}\right. \tag{43}$$

4.1.12. The derivative of the term $\tilde{M}_{mk} \equiv \tilde{M}_{mk}(\tilde{\Sigma}^\star,\tilde{\mathbf{M}}^\star)$

We know that

$$\tilde{M}_{mk} = R_1\tilde{M}^{\star\star}_{mk} \quad \text{where} \quad R_1 = \sqrt{\frac{M_I}{M^{\star\star}_I}} = \frac{\tilde{\Sigma}_{eq}}{\tilde{\Sigma}_{eq} + \dfrac{3\lambda+2\mu}{45\mu}A_I(\tilde{\Sigma}^\star_{eq}-\tilde{\Sigma}_{eq})} = \frac{\tilde{\Sigma}_{eq}}{\mathcal{D}_1}; \tag{44}$$

as a consequence, we get

$$\left\{\begin{array}{l}
\dfrac{\partial R_1}{\partial\tilde{\Sigma}^\star_{pq}} = \dfrac{1}{\mathcal{D}_1}\dfrac{D\tilde{\Sigma}_{eq}}{D\tilde{\Sigma}^\star_{pq}} - \dfrac{\tilde{\Sigma}_{eq}}{\mathcal{D}_1^2}\left(\dfrac{\partial\mathcal{D}_1}{\partial\tilde{\Sigma}^\star_{pq}} + \dfrac{\partial\mathcal{D}_1}{\partial\tilde{\Sigma}_{eq}}\dfrac{D\tilde{\Sigma}_{eq}}{D\tilde{\Sigma}^\star_{pq}}\right) \\
\dfrac{\partial R_1}{\partial\tilde{M}^\star_{pqr}} = \dfrac{1}{\mathcal{D}_1}\dfrac{D\tilde{\Sigma}_{eq}}{D\tilde{M}^\star_{pqr}} - \dfrac{\tilde{\Sigma}_{eq}}{\mathcal{D}_1^2}\dfrac{\partial\mathcal{D}_1}{\partial\tilde{\Sigma}_{eq}}\dfrac{D\tilde{\Sigma}_{eq}}{D\tilde{M}^\star_{pqr}}.
\end{array}\right. \tag{45}$$

Thereafter, we obtain

$$\frac{\partial\tilde{M}_{mk}}{\partial\Sigma^\star_{pq}} = R_2\frac{D\tilde{M}^{\star\star}_{mk}}{D\tilde{\Sigma}^\star_{pq}} + \frac{\partial R_1}{\partial\tilde{\Sigma}^\star_{pq}}M^{\star\star}_{mk} \quad ; \quad \frac{\partial\tilde{M}_{mk}}{\partial M^\star_{pqr}} = R_1\frac{D\tilde{M}^{\star\star}_{mk}}{D\tilde{M}^\star_{pqr}} + \frac{\partial R_1}{\partial\tilde{M}^\star_{pqr}}M^{\star\star}_{mk}. \tag{46}$$

Similarily, the fact that

$$\tilde{M}'_{ijk} = R_1 \tilde{M}^{\star\star}{}'_{ijk} \quad \text{where} \quad R_2 = \sqrt{\frac{M_{II}}{M^{\star\star}_{II}}} = \frac{\tilde{\Sigma}_{eq}}{\tilde{\Sigma}_{eq} + \dfrac{A_{II}}{5}(\tilde{\Sigma}^{\star}_{eq} - \tilde{\Sigma}_{eq})} = \frac{\tilde{\Sigma}_{eq}}{\mathcal{D}_2} \tag{47}$$

yields

$$\begin{cases} \dfrac{\partial R_2}{\partial \tilde{\Sigma}^{\star}_{pq}} = \dfrac{1}{\mathcal{D}_2}\dfrac{D\tilde{\Sigma}_{eq}}{D\tilde{\Sigma}^{\star}_{pq}} - \dfrac{\tilde{\Sigma}_{eq}}{\mathcal{D}_2^2}\left(\dfrac{\partial \mathcal{D}_2}{\partial \tilde{\Sigma}^{\star}_{pq}} + \dfrac{\partial \mathcal{D}_2}{\partial \tilde{\Sigma}_{eq}}\dfrac{D\tilde{\Sigma}_{eq}}{D\tilde{\Sigma}^{\star}_{pq}}\right) \\ \dfrac{\partial R_2}{\partial \tilde{M}^{\star}_{pqr}} = \dfrac{1}{\mathcal{D}_2}\dfrac{D\tilde{\Sigma}_{eq}}{D\tilde{M}^{\star}_{pqr}} - \dfrac{\tilde{\Sigma}_{eq}}{\mathcal{D}_2^2}\dfrac{\partial \mathcal{D}_2}{\partial \tilde{\Sigma}_{eq}}\dfrac{D\tilde{\Sigma}_{eq}}{D\tilde{M}^{\star}_{pqr}} \end{cases} \tag{48}$$

which is equivalent to

$$\frac{\partial \tilde{M}'_{ijk}}{\partial \Sigma^{\star}_{pq}} = R_2 \frac{D\tilde{M}^{\star\star}{}'_{ijk}}{D\tilde{\Sigma}^{\star}_{pq}} + \frac{\partial R_2}{\partial \tilde{\Sigma}^{\star}_{pq}} M^{\star\star}_{ijk}{}' \quad ; \quad \frac{\partial \tilde{M}'_{ijk}}{\partial M^{\star}_{pqr}} = R_2 \frac{D\tilde{M}^{\star\star}{}'_{ijk}}{D\tilde{M}^{\star}_{pqr}} + \frac{\partial R_2}{\partial \tilde{M}^{\star}_{pqr}} M^{\star\star}_{ijk}{}'. \tag{49}$$

We easily derive from these equations, the expressions of the derivatives: $\dfrac{\partial \tilde{M}_{ijk}}{\partial \tilde{\Sigma}^{\star}_{pq}}$ and $\dfrac{\partial \tilde{M}_{ijk}}{\partial \tilde{M}^{\star}_{pqr}}$. We specify that

$$\begin{cases} \tilde{M}_I = \dfrac{\tilde{M}^{\star\star}_I \tilde{\Sigma}^2_{eq}}{\left(\tilde{\Sigma}_{eq} + \dfrac{3\lambda + 2\mu}{45\mu} A_I (\tilde{\Sigma}^{\star}_{eq} - \tilde{\Sigma}_{eq})\right)^2} = R_1^2 \tilde{M}^{\star\star}_I \\ \tilde{M}_{II} = R_2^2 \tilde{M}^{\star\star}_{II}, \end{cases} \tag{50}$$

$$\begin{cases} \dfrac{\partial \tilde{M}_I}{\partial \tilde{\Sigma}^{\star}_{pq}} = 2R_1 \dfrac{\partial R_1}{\partial \tilde{\Sigma}^{\star}_{pq}} \tilde{M}^{\star\star}_I + R_1^2 \dfrac{D\tilde{M}^{\star\star}_I}{D\tilde{\Sigma}^{\star}_{pq}} \\ \dfrac{\partial \tilde{M}_{II}}{\partial \tilde{\Sigma}^{\star}_{pq}} = 2R_2 \dfrac{\partial R_2}{\partial \tilde{\Sigma}^{\star}_{pq}} \tilde{M}^{\star\star}_{II} + R_2^2 \dfrac{D\tilde{M}^{\star\star}_{II}}{D\tilde{\Sigma}^{\star}_{pq}} \end{cases} \quad \text{with} \quad \begin{cases} \dfrac{D\tilde{M}^{\star\star}_I}{D\tilde{\Sigma}^{\star}_{pq}} = \dfrac{\partial \tilde{M}^{\star\star}_I}{\partial \tilde{\Sigma}^{\star}_{pq}} + \dfrac{\partial \tilde{M}^{\star\star}_I}{\partial \tilde{\Sigma}_{eq}} \dfrac{D\tilde{\Sigma}_{eq}}{D\tilde{\Sigma}^{\star}_{pq}} \\ \dfrac{D\tilde{M}^{\star\star}_{II}{}'}{D\tilde{\Sigma}^{\star}_{pq}} = \dfrac{\partial \tilde{M}^{\star\star}_{II}{}'}{\partial \tilde{\Sigma}^{\star}_{pq}} + \dfrac{\partial \tilde{M}^{\star\star}_{II}{}'}{\partial \tilde{\Sigma}_{eq}} \dfrac{D\tilde{\Sigma}_{eq}}{D\tilde{\Sigma}^{\star}_{pq}}. \end{cases} \tag{51}$$

4.1.13. Introduction of work hardening and transition to non-reduced stresses

The equation giving $\Delta\bar{\varepsilon}$, written with "reduced" constraints and moments, is:

$$\begin{aligned} (1-f)\frac{\Delta\bar{\varepsilon}}{\bar{\Sigma}} &= \tilde{\Sigma}_{eq}\frac{\tilde{\Sigma}^{\star}_{eq} - \tilde{\Sigma}_{eq}}{3\mu} + 3\tilde{\Sigma}_m \frac{\tilde{\Sigma}^{\star}_m - \tilde{\Sigma}_m}{3\lambda + 2\mu} + \\ &+ \tilde{M}'_{ijk}\frac{\tilde{M}^{\star}_{ijk}{}' - \tilde{M}'_{ijk}}{2\mu b^2/5} + 3\tilde{M}_{mk}\frac{\tilde{M}^{\star}_{mk} - \tilde{M}_{mk}}{(3\lambda + 2\mu)b^2/5} \end{aligned}$$

which can also be written as:

$$\begin{aligned} (1-f)\frac{\Delta\bar{\varepsilon}}{\bar{\Sigma}} &= \tilde{\Sigma}'_{ij}\frac{\tilde{\Sigma}^{\star}_{ij}{}' - \tilde{\Sigma}'_{ij}}{2\mu} + 3\tilde{\Sigma}_m \frac{\tilde{\Sigma}^{\star}_m - \tilde{\Sigma}_m}{3\lambda + 2\mu} + \\ &+ \tilde{M}'_{ijk}\frac{\tilde{M}^{\star}_{ijk}{}' - \tilde{M}'_{ijk}}{2\mu b^2/5} + 3\tilde{M}_{mk}\frac{\tilde{M}^{\star}_{mk} - \tilde{M}_{mk}}{(3\lambda + 2\mu)b^2/5} \end{aligned}$$

Differentiating the last expression Eq.(52) by considering small variations of $\tilde{\Sigma}^{\star}_{pq}$ and $\tilde{M}^{\star}_{pqr}$, we get

$$\begin{aligned} D\left[(1-f)\frac{\Delta\bar{\varepsilon}}{\bar{\Sigma}}\right] &= (1-f)\left[\frac{D\Delta\bar{\varepsilon}}{\bar{\Sigma}} - \frac{\Delta\bar{\varepsilon}}{\bar{\Sigma}^2}D\bar{\Sigma}\right] \\ &= \frac{1-f}{\bar{\Sigma}}(\frac{1}{h} - \frac{\Delta\bar{\varepsilon}}{\bar{\Sigma}})D\bar{\Sigma} \end{aligned}$$

where

$$h = \frac{D\bar{\Sigma}}{D\bar{\varepsilon}}.$$

Thus, we obtain

$$\begin{aligned} \frac{1-f}{\bar{\Sigma}}(\frac{1}{h} - \frac{\Delta\bar{\varepsilon}}{\bar{\Sigma}})D\bar{\Sigma} &= D\tilde{\Sigma}'_{ij}\frac{\tilde{\Sigma^{\star}_{ij}}' - \tilde{\Sigma}'_{ij}}{2\mu} + 3D\tilde{\Sigma}_m\frac{\tilde{\Sigma}^{\star}_m - \tilde{\Sigma}_m}{3\lambda+2\mu} \\ &+ D\tilde{M}'_{ijk}\frac{\tilde{M^{\star}_{ijk}}' - \tilde{M}'_{ijk}}{2\mu b^2/5} + 3D\tilde{M}_{mk}\frac{\tilde{M}^{\star}_{mk} - \tilde{M}_{mk}}{(3\lambda+2\mu)b^2/5} \\ &+ \tilde{\Sigma}'_{ij}\frac{D\tilde{\Sigma^{\star}_{ij}}' - D\tilde{\Sigma}'_{ij}}{2\mu} + \frac{3\tilde{\Sigma}_m}{3\lambda+2\mu}(D\tilde{\Sigma}^{\star}_m - D\tilde{\Sigma}_m) \\ &+ \tilde{M}'_{ijk}\frac{D\tilde{M^{\star}_{ijk}}' - D\tilde{M}'_{ijk}}{2\mu b^2/5} + 3\tilde{M}_{mk}\frac{D\tilde{M}^{\star}_{mk} - D\tilde{M}_{mk}}{(3\lambda+2\mu)b^2/5} \end{aligned}$$

The sum of the first four terms is zero. Indeed, this sum can be written as

$$D\tilde{\Sigma}'_{ij}\Delta\tilde{\varepsilon^p_{ij}}' + 3\mathrm{d}\tilde{\Sigma}_m\Delta\tilde{\varepsilon}^p_m + D\tilde{M}'_{ijk}\Delta(\nabla\tilde{w})^p_{ijk}{}' + 3D\tilde{M}_{mk}(\nabla\tilde{w})^p_{mk} = D\tilde{\Sigma}_{ij}\Delta\tilde{\varepsilon}^p_{ij} + D\tilde{M}_{ijk}\Delta(\nabla\tilde{w})^p_{ijk}.$$

Yet, the plasticity criterion of Gologanu *et al.* can be written in the form

$$\tilde{\Phi}(\tilde{\mathbf{\Sigma}},\tilde{\mathbf{M}}) = 0 \quad \Rightarrow \quad \frac{\partial\tilde{\Phi}}{\partial\tilde{\Sigma}_{ij}}D\tilde{\Sigma}_{ij} + \frac{\partial\tilde{\Phi}}{\partial\tilde{M}_{ijk}}D\tilde{M}_{ijk} = 0 \quad \text{and} \quad \Delta\tilde{\epsilon}^p_{ij} = \Delta\tilde{\eta}\frac{\partial\tilde{\Phi}}{\partial\tilde{\Sigma}_{ij}} \quad ,$$

$$\Delta(\nabla\tilde{w})^p_{ijk} = \Delta\tilde{\eta}\left(\frac{\partial\tilde{\Phi}}{\partial\tilde{M}_{ijk}} + \delta_{ik}\tilde{U}_j + \delta_{jk}\tilde{U}_i\right).$$

As a consequence,

$$\Delta\tilde{\varepsilon}^p_{ij}D\tilde{\Sigma}_{ij} + \Delta(\nabla\tilde{w})^p_{ijk}D\tilde{M}_{ijk} = \Delta\tilde{\eta}\left(\frac{\partial\tilde{\Phi}}{\partial\tilde{\Sigma}_{ij}}D\tilde{\Sigma}_{ij} + \frac{\partial\tilde{\Phi}}{\partial\tilde{M}_{ijk}}D\tilde{M}_{ijk} + \delta_{ik}\tilde{U}_jD\tilde{M}_{ijk} + \delta_{jk}\tilde{U}_iD\tilde{M}_{ijk}\right) = 0$$

since

$$D\tilde{M}_{ijj} = 0.$$

4.1.14. The derivatives of $\bar{\Sigma}$ with respect to $\tilde{\Sigma}^\star_{pq}$ and $\tilde{M}^\star_{pqr}$

. We get

$$\left\{\begin{array}{rcl}
\frac{1-f}{\bar{\Sigma}}\left(\frac{1}{h}-\frac{\Delta\bar{\varepsilon}}{\bar{\Sigma}}\right)\frac{\partial\bar{\Sigma}}{\partial\tilde{\Sigma}^\star_{pq}} &=& \frac{\tilde{\Sigma}'_{ij}}{2\mu}\left(\frac{\partial\tilde{\Sigma}^\star_{ij}{}'}{\partial\tilde{\Sigma}^\star_{pq}}-\frac{\partial\tilde{\Sigma}'_{ij}}{\partial\tilde{\Sigma}^\star_{pq}}\right)+\frac{3\tilde{\Sigma}_m}{3\lambda+2\mu}\left(\frac{\partial\tilde{\Sigma}^\star_m}{\partial\tilde{\Sigma}^\star_{pq}}-\frac{\partial\tilde{\Sigma}_m}{\partial\tilde{\Sigma}^\star_{pq}}\right)\\
&-& \frac{\tilde{M}'_{ijk}}{2\mu b^2/5}\frac{\partial\tilde{M}_{ijk}{}'}{\tilde{\partial}\Sigma^\star_{pq}}-3\frac{\tilde{M}_{mk}}{(3\lambda+2\mu)b^2/5}\frac{\partial\tilde{M}_{mk}}{\tilde{\partial}\Sigma^\star_{pq}}\\
&=& \frac{\tilde{\Sigma}'_{ij}}{2\mu}\left[\frac{1}{2}(\delta_{ip}\delta_{jq}+\delta_{iq}\delta_{jp})-\frac{1}{3}\delta_{ij}\delta_{pq}\right]-\frac{1}{6\mu}\frac{\mathrm{D}\tilde{\Sigma}^2_{eq}}{\mathrm{D}\tilde{\Sigma}^\star_{pq}}\\
&+& \frac{3\tilde{\Sigma}_m}{3\lambda+2\mu}\frac{1}{3}\delta_{pq}-3\frac{\tilde{\Sigma}_m}{3\lambda+2\mu}\frac{\partial\tilde{\Sigma}_m}{\partial\tilde{\Sigma}^\star_{pq}}\\
&-& \frac{1}{6\mu b^2/5}\frac{\partial\tilde{M}_{II}}{\partial\tilde{\Sigma}^\star_{pq}}-3\frac{\tilde{M}_{mk}}{(3\lambda+2\mu)b^2/5}\frac{\partial\tilde{M}_{mk}}{\partial\tilde{\Sigma}^\star_{pq}}\\
&=& \frac{\tilde{\Sigma}'_{pq}}{2\mu}-\frac{\tilde{\Sigma}_{eq}}{3\mu}\frac{\mathrm{D}\tilde{\Sigma}_{eq}}{\mathrm{D}\tilde{\Sigma}^\star_{pq}}+\frac{\tilde{\Sigma}_m}{3\lambda+2\mu}\delta_{pq}-3\frac{\tilde{\Sigma}_m}{3\lambda+2\mu}\frac{\partial\tilde{\Sigma}_m}{\partial\tilde{\Sigma}^\star_{pq}}\\
&-& \frac{1}{6\mu b^2/5}\frac{\partial\tilde{M}_{II}}{\partial\tilde{\Sigma}^\star_{pq}}-\frac{3}{2(3\lambda+2\mu)b^2/5}\frac{\partial\tilde{M}_I}{\partial\tilde{\Sigma}^\star_{pq}}.
\end{array}\right. \tag{52}$$

Similarily, we find

$$\left\{\begin{array}{rcl}
\frac{1-f}{\bar{\Sigma}}\left(\frac{1}{h}-\frac{\Delta\bar{\varepsilon}}{\bar{\Sigma}}\right)\frac{\partial\bar{\Sigma}}{\partial\tilde{M}^\star_{pqr}} &=& -\frac{\tilde{\Sigma}'_{ij}}{2\mu}\frac{\partial\tilde{\Sigma}'_{ij}}{\partial\tilde{M}^\star_{pqr}}-\frac{3\tilde{\Sigma}_m}{3\lambda+2\mu}\frac{\partial\tilde{\Sigma}_m}{\partial\tilde{M}^\star_{pqr}}\\
&+& \frac{\tilde{M}'_{ijk}}{2\mu b^2/5}\left[\frac{1}{2}(\delta_{ip}\delta_{jq}+\delta_{iq}\delta_{jp})-\frac{1}{3}\delta_{ij}\delta_{pq}\right]\delta_{kr}\\
&-& \frac{\tilde{M}'_{ijk}}{2\mu b^2/5}\frac{\partial\tilde{M}_{ijk}{}'}{\partial\tilde{M}^\star_{pqr}}+3\frac{\tilde{M}_{mk}}{(3\lambda+2\mu)b^2/5}\frac{1}{3}\delta_{pq}\delta_{kr}\\
&-& 3\frac{\tilde{M}_{mk}}{(3\lambda+2\mu)b^2/5}\frac{\partial\tilde{M}_{mk}}{\partial\tilde{M}^\star_{pqr}}\\
&=& -\frac{\tilde{\Sigma}_{eq}}{3\mu}\frac{\mathrm{D}\tilde{\Sigma}_{eq}}{D\tilde{M}^\star_{pqr}}+\frac{\tilde{M}_{mr}}{(3\lambda+2\mu)b^2/5}\delta_{pq}-3\frac{\tilde{\Sigma}_m}{3\lambda+2\mu}\frac{\partial\tilde{\Sigma}_m}{\partial\tilde{M}^\star_{pqr}}\\
&-& \frac{1}{6\mu b^2/5}\frac{\partial\tilde{M}_{II}}{\partial\tilde{M}^\star_{pqr}}-\frac{3}{2(3\lambda+2\mu)b^2/5}\frac{\partial\tilde{M}_I}{\partial\tilde{M}^\star_{pqr}}+\frac{\tilde{M}'_{pqr}}{2\mu b^2/5}.
\end{array}\right. \tag{53}$$

4.1.15. The derivatives of $\bar{\Sigma}$ with respect $\Sigma^\star_{pq}$ and $M^\star_{pqr}$

We determine the expression of the non-normalized stresses and moments by:

$$\begin{array}{rcl}
\bar{\Sigma} &\equiv& \bar{\Sigma}(\tilde{\mathbf{\Sigma}}^\star,\mathbf{M}^\star)\equiv\bar{\Sigma}(\frac{\tilde{\mathbf{\Sigma}}^\star}{\bar{\Sigma}},\frac{\mathbf{M}^\star}{\bar{\Sigma}})\\
&\Rightarrow& D\bar{\Sigma}=\frac{\partial\bar{\Sigma}}{\partial\tilde{\Sigma}^\star_{pq}}\left(\frac{D\Sigma^\star_{pq}}{\bar{\Sigma}}-\frac{\Sigma^\star_{pq}}{\bar{\Sigma}^2}D\bar{\Sigma}\right)+\frac{\partial\bar{\Sigma}}{\partial\tilde{M}^\star_{pqr}}\left(\frac{DM^\star_{pqr}}{\bar{\Sigma}}-\frac{M^\star_{pqr}}{\bar{\Sigma}^2}D\bar{\Sigma}\right)
\end{array}$$

$$\Rightarrow \quad \left(1+\frac{1}{\bar{\Sigma}^2}\frac{\partial\bar{\Sigma}}{\partial\tilde{\Sigma}^\star_{pq}}\Sigma^\star_{pq}+\frac{1}{\bar{\Sigma}^2}\frac{\partial\bar{\Sigma}}{\partial\tilde{M}^\star_{pqr}}M^\star_{pqr}\right)D\bar{\Sigma}=\frac{1}{\bar{\Sigma}}\frac{\partial\bar{\Sigma}}{\partial\tilde{\Sigma}^\star_{pq}}D\Sigma^\star_{pq}+\frac{1}{\bar{\Sigma}}\frac{\partial\bar{\Sigma}}{\partial\tilde{M}^\star_{pqr}}DM^\star_{pqr}.$$

Finally, we obtain

$$\begin{cases} \dfrac{\partial\bar{\Sigma}}{\partial\Sigma^\star_{pq}}=\dfrac{\dfrac{1}{\bar{\Sigma}}\dfrac{\partial\bar{\Sigma}}{\partial\tilde{\Sigma}^\star_{pq}}}{1+\dfrac{1}{\bar{\Sigma}^2}\dfrac{\partial\bar{\Sigma}}{\partial\Sigma^\star_{ij}}\Sigma^\star_{ij}+\dfrac{1}{\bar{\Sigma}^2}\dfrac{\partial\bar{\Sigma}}{\partial\partial M^\star_{ijk}}M^\star_{ijk}} \\ \dfrac{\partial\bar{\Sigma}}{\partial M^\star_{pqr}}=\dfrac{\dfrac{1}{\bar{\Sigma}}\dfrac{\partial\bar{\Sigma}}{\partial\tilde{M}^\star_{pqr}}}{1+\dfrac{1}{\bar{\Sigma}^2}\dfrac{\partial\bar{\Sigma}}{\partial\tilde{\Sigma}^\star_{ij}}\Sigma^\star_{ij}+\dfrac{1}{\bar{\Sigma}^2}\dfrac{\partial\bar{\Sigma}}{\partial\tilde{M}^\star_{ijk}}M^\star_{ijk}}. \end{cases} \tag{54}$$

We had $\Sigma_{ij}\equiv\bar{\Sigma}(\mathbf{\Sigma}^\star,\mathbf{M}^\star)\tilde{\Sigma}_{ij}(\dfrac{\mathbf{\Sigma}^\star}{\bar{\Sigma}},\dfrac{\mathbf{M}^\star}{\bar{\Sigma}})$; and it follows that

$$\begin{aligned} D\Sigma_{ij} &= D\bar{\Sigma}\tilde{\Sigma}_{ij}+\bar{\Sigma}\frac{\partial\tilde{\Sigma}_{ij}}{\partial\tilde{\Sigma}^\star_{pq}}\left(\frac{D\Sigma^\star_{pq}}{\bar{\Sigma}}-\frac{\Sigma^\star_{pq}}{\bar{\Sigma}^2}D\bar{\Sigma}\right)+\bar{\Sigma}\frac{\partial\tilde{\Sigma}_{ij}}{\partial\tilde{M}^\star_{pqr}}\left(\frac{DM^\star_{pqr}}{\bar{\Sigma}}-\frac{M^\star_{pqr}}{\bar{\Sigma}^2}D\bar{\Sigma}\right) \\ &= \left(\tilde{\Sigma}_{ij}-\frac{\partial\tilde{\Sigma}_{ij}}{\partial\tilde{\Sigma}^\star_{hk}}\frac{\Sigma^\star_{hk}}{\bar{\Sigma}}-\frac{\partial\tilde{\Sigma}_{ij}}{\partial\tilde{M}^\star_{hkl}}\frac{M^\star_{hkl}}{\bar{\Sigma}}\right)\left(\frac{\partial\bar{\Sigma}}{\partial\Sigma^\star_{pq}}D\Sigma^\star_{pq}+\frac{\partial\bar{\Sigma}}{\partial\tilde{M}^\star_{pqr}}DM^\star_{pqr}\right) \\ &+ \frac{\partial\tilde{\Sigma}_{ij}}{\partial\tilde{\Sigma}^\star_{pq}}D\Sigma^\star_{pq}+\frac{\partial\tilde{\Sigma}_{ij}}{\partial\tilde{M}^\star_{pqr}}DM^\star_{pqr}. \end{aligned}$$

Thereafter, we obtain

$$\begin{cases} \dfrac{\partial\Sigma_{ij}}{\partial\Sigma^\star_{pq}}=\left(\tilde{\Sigma}_{ij}-\dfrac{\partial\tilde{\Sigma}_{ij}}{\partial\tilde{\Sigma}^\star_{hk}}\tilde{\Sigma}^\star_{hk}-\dfrac{\partial\tilde{\Sigma}_{ij}}{\partial\tilde{M}^\star_{hkl}}\tilde{M}^\star_{hkl}\right)\dfrac{\partial\bar{\Sigma}}{\partial\Sigma^\star_{pq}}+\dfrac{\partial\tilde{\Sigma}_{ij}}{\partial\tilde{\Sigma}^\star_{pq}} \\ \dfrac{\partial\Sigma_{ij}}{\partial M^\star_{pqr}}=\left(\tilde{\Sigma}_{ij}-\dfrac{\partial\tilde{\Sigma}_{ij}}{\partial\tilde{\Sigma}^\star_{hk}}\tilde{\Sigma}^\star_{hk}-\dfrac{\partial\tilde{\Sigma}_{ij}}{\partial\tilde{M}^\star_{hkl}}\tilde{M}^\star_{hkl}\right)\dfrac{\partial\bar{\Sigma}}{\partial M^\star_{pqr}}+\dfrac{\partial\tilde{\Sigma}_{ij}}{\partial\tilde{M}^\star_{pqr}}. \end{cases} \tag{55}$$

Similarily, $M_{ijk}\equiv\bar{\Sigma}(\mathbf{\Sigma}^\star,\mathbf{M}^\star)\tilde{M}_{ijk}(\dfrac{\mathbf{\Sigma}^\star}{\bar{\Sigma}},\dfrac{\mathbf{M}^\star}{\bar{\Sigma}})$; we deduce that

$$\begin{cases} \dfrac{\partial M_{ijk}}{\partial\Sigma^\star_{pq}}=\left(\tilde{M}_{ijk}-\dfrac{\partial\tilde{M}_{ijk}}{\partial\tilde{\Sigma}^\star_{lm}}\tilde{\Sigma}^\star_{lm}-\dfrac{\partial\tilde{M}_{ijk}}{\partial\tilde{M}^\star_{lmn}}\tilde{M}^\star_{lmn}\right)\dfrac{\partial\bar{\Sigma}}{\partial\Sigma^\star_{pq}}+\dfrac{\partial\tilde{M}_{ijk}}{\partial\tilde{\Sigma}^\star_{pq}} \\ \dfrac{\partial M_{ijk}}{\partial M^\star_{pqr}}=\left(\tilde{M}_{ijk}-\dfrac{\partial\tilde{M}_{ijk}}{\partial\tilde{\Sigma}^\star_{lm}}\tilde{\Sigma}^\star_{lm}-\dfrac{\partial\tilde{M}_{ijk}}{\partial\tilde{M}^\star_{lmn}}\tilde{M}^\star_{lmn}\right)\dfrac{\partial\bar{\Sigma}}{\partial M^\star_{pqr}}+\dfrac{\partial\tilde{M}_{ijk}}{\partial\tilde{M}^\star_{pqr}}. \end{cases} \tag{56}$$

4.1.16. The derivatives of Σ_{ij} and M_{ijk} with respect to $\Delta\varepsilon_{pq}$ and $\Delta(\nabla W)_{pqr}$

We obtain

$$\left\{\begin{array}{ll} \dfrac{\partial\Sigma_{ij}}{\partial\Delta\varepsilon_{pq}} = \dfrac{\partial\Sigma_{ij}}{\partial\Sigma^{\star}_{lm}}\dfrac{\partial\Sigma^{\star}_{lm}}{\partial\Delta\varepsilon_{pq}} & ; \quad \dfrac{\partial\Sigma_{ij}}{\Delta(\nabla W)_{pqr}} = \dfrac{\partial\Sigma_{ij}}{\partial M^{\star}_{lmn}}\dfrac{\partial M^{\star}_{lmn}}{\partial\Delta(\nabla W)_{pqr}} \\ \dfrac{\partial M_{ijk}}{\partial\Delta\varepsilon_{pq}} = \dfrac{\partial M_{ijk}}{\partial\Sigma^{\star}_{lm}}\dfrac{\partial\Sigma^{\star}_{lm}}{\partial\Delta\varepsilon_{pq}} & ; \quad \dfrac{\partial M_{ijk}}{\Delta(\nabla W)_{pqr}} = \dfrac{\partial M_{ijk}}{\partial M^{\star}_{lmn}}\dfrac{\partial M^{\star}_{lmn}}{\Delta(\nabla W)_{pqr}}. \end{array}\right. \tag{57}$$

5. Assessment of the approach

5.1. Simulations of an axisymmetric notched specimen loaded in tension

We have implemented the developed tangent stiffness matrix for the GLPD model using Systus® finite element software developed by ESI group. To test the procedure we simulate a tensile test on an axisymmetric notched specimen in A508 Cl.3 steel, for which the mechanical fields (stresses and deformations) are homogeneous in the ligament of the specimen.

In each of the simulations, we use the value of the Tvergaard parameter $q = 4/e = 1.47$ determined by Perrin and Leblond [18] by a "differential' scheme '. The A508 Cl.3 steel is used in the design of reactor vessels for nuclear power plants. For this steel, the Young's modulus is worth $E = 203000$ MPa, the Poisson's ratio $\nu = 0.3$, and the initial yield stress in simple tension $\Sigma_y = 450$ MPa. The value of the initial porosity f_0 of this steel comes from the study of its chemical composition and its inclusionary state, see [21] . The value of f_0 is deduced from the sulfur and manganese content of the material and the average dimensions of the inclusions. The value found is $f_0 = 0.00016$. To this damage parameter are added two others, f_c and δ, respectively representing the critical porosity at the start of coalescence and the accelerating factor of the growth of the cavities whose values can be adjusted from one simulation to another.

The notch radius of this specimen is $5mm$. The specimen used is cylindrical. The symmetry and axisymmetry of the problem are exploited to model only a quarter of a longitudinal section of the specimen. The nodes located in the minimum section are axially locked in the direction Y; the loading of the specimen is a displacement applied to all the nodes of the upper surface of the discretized sample portion, varying linearly over time. The numerical calculations are carried out with meshes whose dimensions are worth $0.4 \times 0.2mm^2$ in the region of the ligament, for a characteristic distance b of 10^{-5} μm. The mesh of this specimen is given in Figure 1. Figure 2 shows the sum of the nodal force for the nodes located in the upper face of the specimen vs. time curves obtained with the Gurson model and the GLPD model. In this specific case, we do not make a comparison with experiments because we do not have experimental results for this type of specimen. On the other hand, we compare between them the curves obtained with the local Gurson models and the GLPD model for a characteristic distance $b = 0.00001\mu$m . These simulations indicate that for values of the characteristic distance tending toward 0, we find the force/displacement curve obtained with the local Gurson's model. These comparisons seem to indicate that the numerical results are going in the right direction and allow us to continue the tests on specimen geometries where the stress and strain gradients are large. Note that quadratic convergence of elasto-plastic iterations were obtained without using the stiffness matrix relations we discussed in the previous sections. The situation will be different with the simulations of ductile fracture of pre-cracked specimens.

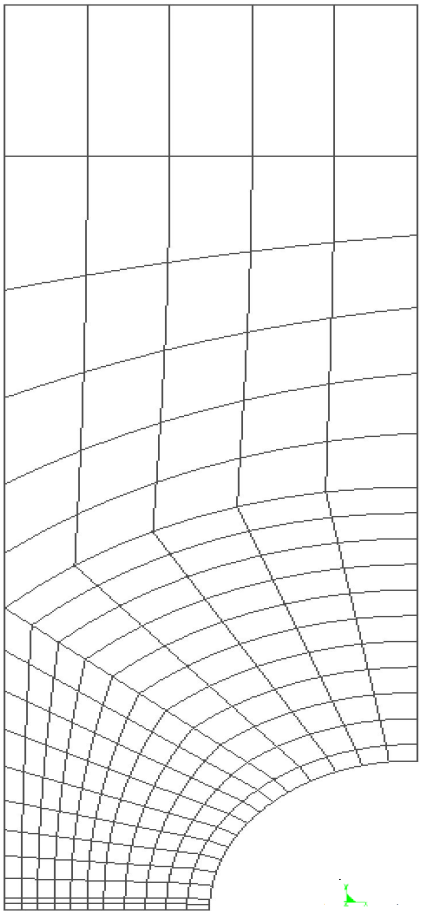

Figure 1: *Mesh of the AE05 Specimen. The dimensions of the meshes are worth* $0.4 \times 0.2 mm^2$ *in the region of the ligament.*

5.2. Simulations of pre-cracked specimens

We now perform an axisymmetric simulation of fracture test of a tensile pre-cracked specimen TA15 in A508 Cl.3 steel, for which we have experimental results. The geometry of the specimen and its discretization are represented in Figure 4. We take advantage of the conditions of symmetry and axisymmetry by modeling only a quarter of a longitudinal section of the specimen with again quadrangle elements (8 nodes and 4 Gaussian points per sub-integrated element). The few triangular elements, unavoidable in the automatic generation of the mesh, have no effect on the result because they are located outside the sensitive zone of this problem (area of the crack tip and region ahead of the crack tip). The values of the half-height and the radius of the TA15 specimen are 22.5 mm and 15 mm, respectively. The half-angle of the opening is worth 15°; the depth of the central V-shaped notch is 3.88 mm. The pre-cracking radius is taken equal to 4 mm. A crack develops from the tip of this pre-crack and propagates toward the axis of rotational symmetry. The values of the material parameters are the same as the ones used in the case of the simulations of an axisymmetric notched specimen loaded in tension and presented above.

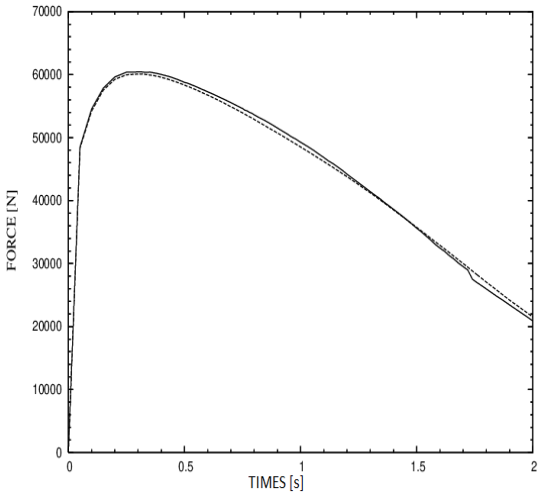

Figure 2: *Time history of the sum of the nodal force for the nodes located in the upper face of the specimen. Full line: Gurson model; dashed line: GLPD model*

Behind the crack, the discretization radiates with an angular sector divided into 4 to properly represent the significant stress and strain gradients in this area. Among the four meshes adjoining the crack tip whose intermediate nodes are pushed back to the quarter, we distinguish two quasi-degenerate quadrilaterals and two triangles. The role of the first meshes is to enable the representation of the blunting; the quasi-merged nodes deviate during the deformation. In front of the crack, the discretization comprises identical square elements, see Figure 3. The numerical results are obtained using the GLPD model

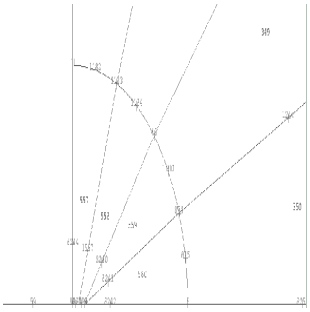

Figure 3: *Mesh at the tip of the crack with 4 meshes whose nodes are pushed back to the quarter*

with a characteristic distance $b = 550\,\mu$m for a mesh size of $200\,\mu$m in the region of the ligament and accounting for the stiffness matrix. The simulations on the TA15 specimen could not be completed satisfactorily. Indeed, it was difficult to obtain the convergence of numerical calculations beyond a certain level of loading as indicated in Figure5 which displays the experimental and numerical force/displacement

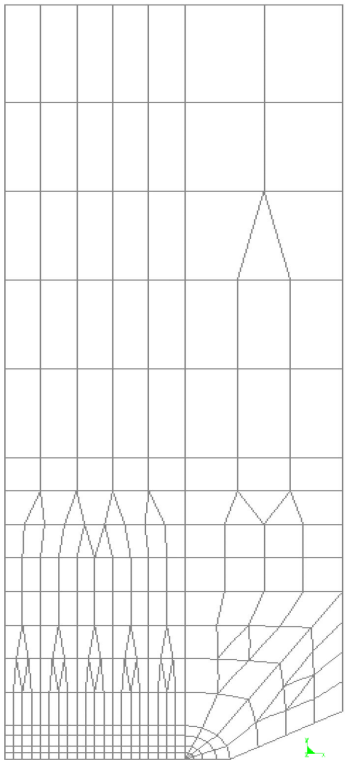

Figure 4: *Mesh of the TA15 specimen. The values of the half-height and the radius of the TA15 specimen are 22.5 mm and 15 mm. The half-angle of the opening is worth* $15°$*; the depth of the central V-shaped notch is 3.88 mm.*

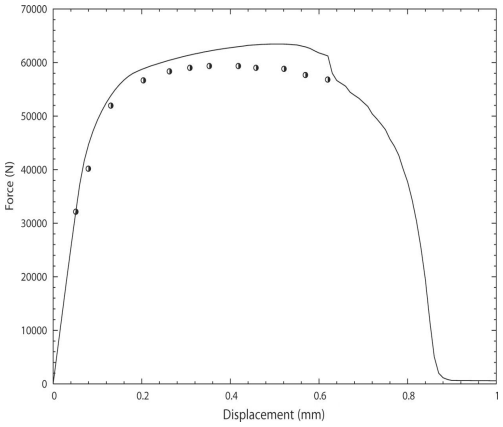

Figure 5: *Comparison between experiments and numerical simulations. Force/displacement curves for a TA15 specimen for a mesh size* $200\,\mu m$ *in the ligament ahead of the crack tip and a characteristic distance* $b = 550\,\mu m$*: finite element calculations with the GLPD model with tangent stiffness matrix (full line) and experiments (points)*

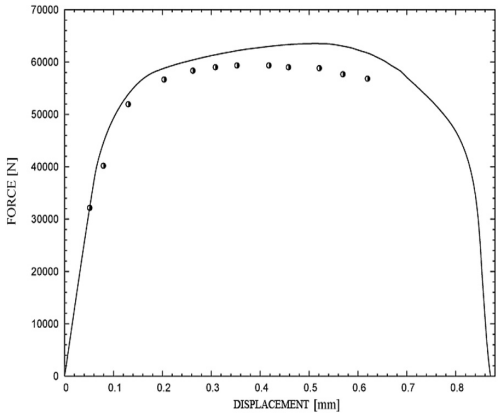

Figure 6: *Comparison between experiments and numerical simulations. Force/displacement curves for a TA15 specimen for a mesh size* $200\,\mu m$ *in the ligament ahead of the crack tip and a characteristic distance* $b = 550\,\mu m$*: finite element calculations with the modified GLPD model algorithm (full line) and experiments (points).*

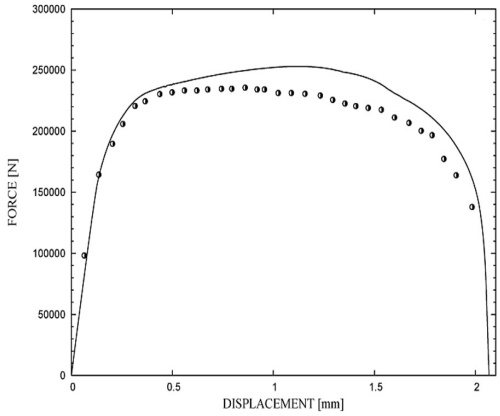

Figure 7: *Comparison between experiments and numerical simulations. Force/displacement curves for a TA130 specimen for a mesh size* $200\,\mu m$ *in the ligament ahead of the crack tip and a characteristic distance* $b = 550\,\mu m$*: finite element calculations with the modified GLPD model algorithm (full line) and experiments (points).*

curves. These convergence difficulties are illustrated on Figure 5 by the non-smoothness of the predicted force/displacement curve around 60% of displacement (a slight bump appears); in all probability this bump happens when the accumulation of damage becomes important. Also, the simulations on a TA30 specimen[4] could not be completed beyound a certain level of loading: the calculations simply stop. The same convergence issues arise if a classical BFGS[5] method [2] algorithm is used for the numerical sim-

[4]The height and diameter of the TA30 specimen are 90 *mm* and 30 *mm*, respectively. The central notch is triangular; its opening angle and depth are 60° and 5 *mm* with a pre-crack of length 1.7 *mm* originating from the notch root.

[5]The BFGS acronym stands for Broyden-Fletcher-Goldfarb-Shanno. The BFGS method belongs to a class of quasi-Newton methods that are alternative to forms of Newton-Raphson iteration. These methods consist of updating the

ulations. It is clear that the convergence difficulties with the GLPD model partially originate from the evaluation of spatial derivative of strains, which is a common central point of all numerical implementation of second-gradient models. As we have already explained above, we deduced these derivatives from the newly introduced DOF representing the strains using the first deirvatives of the shape functions, and by enforcing the appropriate coincidence of these new DOF and the strains through some penalty method. The well-known drawbacks of this approach are the increasing number of DOF per node with its consequence on the computation time and care must be taken to select a penalty constant that must be sufficiently large to be efficient, but not too large to generate an ill-conditioned tangent matrix since the set of unknows consist of quantities of distinct dimensions.

The numerical experiment show that the use of the stiffness tangent matrix allows a faster convergence of the global nonlinear problem at each time step (in number of iterations, otherwise in computing time) in cases where a classical BFGS method also leads to convergence, but brings no improvement in the case where the BFGS leads to elasto-plastic convergence issues.

An explicit variant of the elasto-plastic algorithm that does not present these convergence issues (see Figures (6, 7) consists in fixing the values of the increments of plastic deformation and its gradient to those of the previous time step. Thus, these values become known contrary to the first version where they are unknowns of the problem. The resolution of the problem becomes similar to that of a purely elastic problem with initial deformations. If the equilibrium equations are solved on the configuration at t and not at $t + \Delta t$ there remains only a few weak nonlinearities connected to the objective derivatives of the stress and moment tensors. At convergence we recover the converged values of the increments of plastic deformation and its gradient, which we distribute with the algorithm of projection on the criterion into elastic and plastic parts. The projection algorithm is itself unchanged, the existence and uniqueness of the solution therefore remains guarranteed by the mean of the generalized standard character of the GLPD model at fixed porosity, see Enakoutsa *et al.* [3, 5]. The proposed modification is only valid for very small time steps. The error made on the increments of plastic deformation and its gradient is in $\mathcal{O}((\Delta t)^2)$. Indeed, $\Delta \boldsymbol{D}^i = \Delta \boldsymbol{D}^{e_i} + \Delta \boldsymbol{D}^{p_i}$; $\Delta \boldsymbol{D}^i = \Delta \boldsymbol{D}^{e_i} + \Delta \boldsymbol{D}^{p_{i-1}}$, $\Delta \boldsymbol{D}^{p_i} - \Delta \boldsymbol{D}^{p_{i-1}}$ is proportional to $(\Delta t)^2$. For very small $(\Delta t)^2$, $\boldsymbol{D}^{p_i} - \boldsymbol{D}^{p_{i-1}} \to 0$.

coefficient matrix of the finite element method to provide an approximation to the matrix from iteration *(i - 1)* to *i*. The reader interested in the BFGS algorithm can find a full description of this algorithm in [2] . The BFGS algorithm is implemented in Systus finite element code which is used in all the simulations performed in this study.

6. Conclusion

The contributions of this work can be summarized as follows:

- We provide the exact consistent stiffness matrix for a porous material model involving strain-gradient effects, the GLPD model in the framework of small deformations. The expressions for the derivatives of the Cauchy stress tensor and the generalized moment stress tensor the GLPD model involved are derived.
- We have assessed the robustness of the formulation of the stiffness matrix proposed by comparing its numerical predictions with available experimental results of typical ductile fracture tests. The results show that quadratic convergence of the elasto-plastic iterations was obtained by slightly modifying the original algorithm for the GLPD model.

References

[1] Aravas N. (1987). On the numerical integration of a class of pressure-dependent plasticity models, *Int. J. Num. Meth. Engng.*, **24**, 1395-1416.

[2] Bathe, K. (1996). Finite Element Procedure; Prentice-Hall: Upper Saddle River, NJ, USA, 1996

[3] Enakoutsa K., Leblond J.B. and Perrin G. (2007). Numerical implementation and assessment of a phenomenological nonlocal model of ductile rupture, *Comput. Meth. Appl. Mech. Engng.*, **196**, 1946-1957

[4] Enakoutsa K. (2007). Modèle non-locaux en rupture ductile des métaux. Ph.D thesis, Université Pierre et Marie Curie (Paris VI) (in French).

[5] Enakoutsa K., and Leblond J.B. (2009). Numerical implementation and assessment of the GLPD micromorphic model of ductile rupture, *Eur. J. Mech. A/Solids*, **28**, 445-460

[6] Enakoutsa, K., 2012."Some new Applications of the GLPD Micromorphic Model of Ductile Fracture," *Mathematics and Mechanics of Solids,* **19**(3), 242-259

[7] Enakoutsa, K. (2013). Exact results for the problem of a hollow sphere subjected to hydrostatic tension and made of micromorphic plastic porous materials, *Mech. Res. Commun.,* **49**, 1-7

[8] S. Forest, 1998. "Mechanics of generalized continua: construction by homogenization," *J. Phys. IV,* **8**, 39-48.

[9] Forest S., Barbe F. and Cailletaud G. (2000). Cosserat modelling of size effects in the mechanical behaviour of polycrystals and multi-phase materials, *Int. J. Solids Structures*, **37**, 7105-7126.

[10] Gologanu M., Leblond J.B., Perrin G. and Devaux J. (1997). Recent extensions of Gurson's model for porous ductile metals, in: *Continuum Micromechanics*, CISM Courses and Lectures 377, P. Suquet ed., Springer, pp. 61-130

[11] Gurson A.L. (1977). Continuum theory of ductile rupture by void nucleation and growth: Part I - yield criteria and flow rules for porous ductile media, *ASME J. Engng. Mater. Technol.*, **99**, 2-15

[12] Halphen B. and Nguyen Q.S. (1975). Sur les matériaux standards généralisés, *Journal de Mécanique*,

[13] Hill, R., 1967. The essential structure of constitutive laws for metal composites and polycrystals, *Journal of Mechanics and Physics of Solids*, **15**, 79-95

[14] Leblond, J.B., Perrin, G., and Devaux, J.,(1994). Bifurcation Effects in Ductile Metals with Nonlocal Damage, *ASME J. Applied . Mech.*, **6**1, 236-242.

[15] Mandel, J., 1964. Contribution théorique à l'étude de l'écrouissage et des lois d'écoulement plastique, *Proceedings of the 11th International Congress on Applied Mechanics*, Springer, pp. 502-509 (in French)

[16] Matsushima T., Chambon R. and Caillerie D. (2000). Second gradient models as a particular case of microstructured models: a large strain finite element analysis, *Comptes-Rendus Acad. Sc. Paris Série IIb*, **328**, 179-186

[17] Nguyen Q.S. (1977). On the elastic plastic initial-boundary value problem and its numerical integration, *Int. J. Numer. Meth. Engng.*, **11**, 817-832.

[18] Perrin, G, and Leblond, J-B, 1990. Analytical study of a hollow sphere made of plastic porous material and subjected to hydrostatic tension: Application to some problems in ductile fracture of metals,

[19] Perrin, G, and Leblond, JB (2000). Accelerated void growth in porous ductile solids containing two populations of cavities. *Int. J. Plast.,* **16**, 91-120 *Int. J. Plast.,* **6**:677-699

[20] Pijaudier-Cabot, G. and Bazant, Z.P., (1987). Nonlocal Damage Theory, *ASCE J. Engrg. Mech.*, **1**13, 1512-1533

[21] Rousselier, G and Mudry F, 1981. Etude de la Rupture Ductile de l'Acier Faiblement Allie en Mn-Ni-Mo pour Cuves de Reacteurs a Eau Ordinaire sous Pression, Approvisionne sous la forme d'une Debouchure de Tubulure. Resultats du Programme Experimental, EdF Centre des Renardieres Internal Report HT/PV D529 MAT/T43

[22] Shu J., King W. and Fleck N. (1999). Finite elements for materials with strain gradient effects, *Int. J. Numer. Methods Engng.*, **44**, 373-391.

[23] Tvergaard V. (1981). Influence of voids on shear band instabilities under plane strain conditions, *Int. J. Fracture*, **17**, 389-407.

[24] Tvergaard V. and Needleman A. (1984). Analysis of cup-cone fracture in a round tensile bar, *Acta Metall.*, **32**, 157-169

[25] Tvergaard V. and Needleman A.(1997). Nonlocal effects on localization in a void-sheet, *Int. J. Solids Structures,* **34**, 2221-2238

[26] Tvergaard V. and Needleman A. (1995). Effects of nonlocal damage in porous plastic solids, Int. J. Solids Structures, **32**, 1063-1077